

1999

Performance comparison of partially space-time adaptive processing algorithms for airborne radar using MCARM data

Fatma B. Golbasi
Lehigh University

Follow this and additional works at: <http://preserve.lehigh.edu/etd>

Recommended Citation

Golbasi, Fatma B., "Performance comparison of partially space-time adaptive processing algorithms for airborne radar using MCARM data" (1999). *Theses and Dissertations*. Paper 617.

This Thesis is brought to you for free and open access by Lehigh Preserve. It has been accepted for inclusion in Theses and Dissertations by an authorized administrator of Lehigh Preserve. For more information, please contact preserve@lehigh.edu.

Golbasi, Fatma B.

**Performance
Comparison of
Partially Space-
Time Adaptive
Processing
Algorithms...**

January 2000

**PERFORMANCE COMPARISON OF PARTIALLY SPACE-TIME
ADAPTIVE PROCESSING ALGORITHMS FOR
AIRBORNE RADAR USING MCARM DATA**

by

Fatma B. Golbasi

A Thesis

Presented to the Graduate Committee

of Lehigh University

in Candidacy for the Degree of Master of Science

in

Department of Electrical Engineering and Computer Science

Lehigh University

December, 1999

This thesis is accepted in partial fulfillment of the requirements for the degree
of Master of Science.

(Date)

Rick S. Blum
(Professor in Charge)

Department Chairperson

Acknowledgement

I would like to thank my advisor, Prof. Blum for his support and understanding during my studies. I would also like to thank my husband, Hakan Golbasi for his continuous encouragement.

Contents

Acknowledgments	iii
List of Tables	v
List of Figures	vi
Abstract	1
1 Introduction	2
2 Some Reduced Complexity STAP Schemes	6
2.1 General STAP Approach	7
2.2 ADPCA and its beamspace version.....	8
2.3 FTS and subarraying FTS.....	12
2.4 EFA and subarraying EFA.....	13
2.5 Joint-Domain Localized Approach(JDL).....	14
3 Real Data Performance	16
4 Conclusion	38
References	40
Appendix A	42
Biography	43

List Of Tables

1	Test cases for each example.....	17
2	The three best schemes for all the cases when the target is inserted at range 150.....	20
3	The three best schemes for all the cases when the target is inserted at range 350.....	28
4	The three best schemes for all the cases when the target is inserted at range 415.....	36
5	The three best schemes for all the cases when the target is inserted at range 500.....	37
A.1	Parameters for comparison tests in this study.....	42

List Of Figures

1	ADPCA sub-CPA formation.....	10
2	Power spectrum plot of range 150.....	20
3	Performance comparison when target is inserted at range150, case a....	21
4	Performance comparison when target is inserted at range150, case b....	22
5	Performance comparison when target is inserted at range150, case c....	23
6	Performance comparison when target is inserted at range150, case d....	24
7	Performance comparison when target is inserted at range150, case e.....	25
8	Performance comparison when target is inserted at range150, case f.....	26
9	Performance comparison when target is inserted at range150, case g.....	27
10	Power spectrum plot of range 350	28
11	Performance comparison when target is inserted at range 350, case a....	29
12	Performance comparison when target is inserted at range 350, case b...	30
13	Performance comparison when target is inserted at range 350, case c...	31
14	Performance comparison when target is inserted at range 350, case d...	32
15	Performance comparison when target is inserted at range 350, case e....	33
16	Performance comparison when target is inserted at range 350, case f.....	34
17	Performance comparison when target is inserted at range 350, case g....	35
18	Power spectrum plot of range 415	36
19	Power spectrum plot of range 500	37

Abstract

Researchers have developed Space-Time Adaptive Processing (STAP) schemes to cope with the clutter spectral spreading that occurs for a radar mounted on a moving platform. Analysis shows fully adaptive schemes have great potential when tested with simulations of homogeneous environments, but the possible inaccurate estimation of the covariance matrix in a non-homogeneous environment has prompted investigation of partially adaptive STAP (PSTAP) schemes. A general formulation of a PSTAP algorithm is defined and several specific cases are described. Performance is evaluated using a measured data set. The results indicate that the joint-domain localized and the extended factored approach PSTAP algorithms provide good performance while operating in a realistic non-homogeneous environment.

Chapter 1

Introduction

In airborne radar, the detection of targets is often limited by ground clutter and other forms of interference. Platform motion causes Doppler shifts in the ground clutter that makes Doppler filtering alone ineffective. In such cases Space-Time Adaptive Processing (STAP) offers a potential solution.

STAP has been an active research topic for at least the last two decades. Much of the interest was generated by the results in [1] and [2]. Since then several algorithms have been proposed and evaluated using simulated radar data. With the recent improvements in phased array antenna and digital signal processing technology, a STAP-based radar system is becoming an attractive alternative for detection of airborne targets in clutter, as compared to classical low-sidelobe beamforming [3].

Current STAP research efforts [4] are focused on a number of interesting issues. Performance evaluation of several competing STAP approaches is the topic of this thesis. In most previous research, STAP schemes were evaluated using optimistic simulated data or by manipulating stationary platform measurements to simulate motion. While simulated data is very useful in the development and analysis of algorithms, a more complete evaluation includes using actual recorded radar data. Thus, in this thesis, we

compare various STAP schemes using actual measured airborne data. A general formulation of a useful class of STAP processing approaches, which includes most linear processing schemes, is developed which unifies the schemes considered.

Assume the radar transmits a coherent burst of M pulses at a constant pulse repetition frequency $f_r = 1/T_r$, where T_r is the pulse-repetition-interval (PRI). The time interval over which the waveform returns are collected is commonly referred to as the coherent-processing-interval (CPI). The radar antenna used is an array antenna with N identical elements. For each PRI, L time samples are collected to cover the range intervals. Denote the observation corresponding to the i^{th} antenna element at the j^{th} pulse for k^{th} range cell as $\mathbf{x}_{i,j,k}$. It is convenient to denote the part of the datacube which represents the k^{th} range cell of the datacube as

$$\mathbf{X}_k = [\mathbf{x}_{1,1,k}, \mathbf{x}_{2,1,k}, \dots, \mathbf{x}_{N,1,k}, \mathbf{x}_{1,2,k}, \dots, \mathbf{x}_{N,M,k}]^T \quad (1)$$

where \mathbf{a}^T denotes the transpose of the vector \mathbf{a} . We will refer to \mathbf{X}_k as a space-time snapshot.

A simple set of STAP schemes that have been suggested can be represented as an inner product of the conjugate of a weight vector \mathbf{w} and the vector \mathbf{X}_k . This inner product

$$\mathbf{z} = \mathbf{w}^H \mathbf{X}_k \quad (2)$$

produces the complex quantity z whose magnitude is often compared to a threshold to make a decision. The weight vector w may depend on the estimated interference-plus-noise environment and on the target of interest. In the well-known sample matrix inversion (SMI) algorithm [2] for example, a popular fully adaptive algorithm, the weight vector is given, to within a scale factor, as

$$w = R^{-1}V(S) \quad (3)$$

where R is the estimated interference-plus-noise covariance matrix. The estimate is based on a set of reference data, typically chosen from the surrounding range cells. $V(S)$ is the normalized target response (X_k for a target observed without clutter or noise) [5]. In the case where the interference statistics are known or the estimated covariance matrix is exactly equal to the true covariance matrix, SMI can achieve optimal performance. A fully adaptive STAP scheme, like SMI, requires the formation of an NM by NM covariance matrix which can be a problem. Even for moderate M and N , the computational cost of the computation of R^{-1} becomes excessive in real-time implementations. As a result, reduced complexity approaches called partially adaptive STAP (PSTAP) have been developed whose computational cost is substantially smaller. Some examples of reduced complexity approaches are given in the next chapter.

The schemes which estimate the interference-plus-noise statistics typically require a large set of independent and identically distributed (iid) reference data vectors to achieve an accurate estimation. This requirement may be unrealistic, since measurements [6] indicate that multi-channel airborne radar clutter data is often severely non-homogeneous. For this reason the reference data set available for estimation of clutter statistics is usually quite small. Therefore it is important to know how different STAP algorithms perform for such cases.

In Chapter 2 we define a general STAP scheme and give a detailed description of several specific approaches. Performance comparisons based on measured airborne radar data are presented in Chapter 3. Conclusions are given in Chapter 4.

Chapter 2

Some Reduced Complexity STAP Schemes

STAP is an active research area and new schemes are continually being developed. In order to compare schemes, a standard terminology is useful. Here, we will mainly follow the terminology used in [5]. We caution the reader that other terminology also appears in the literature. We first define a general formulation of PSTAP processing approach which encompasses many existing PSTAP algorithms. Next we describe eight specific approaches which are included in the general formulation. They are

1. Adaptive Displaced Phase-Centered Antenna (ADPCA)
2. Subarraying ADPCA (BDPCA)
3. Beamspace ADPCA (BeamAD)
4. Factored Post Doppler (FTS)
5. Subarraying FTS (BFTS)
6. Extended Factored Approach (EFA)
7. Subarraying EFA (BEFA)
8. Joint-domain Localized Approach (JDL)

2.1 General STAP Approach

Consider the transformations

$$\tilde{\mathbf{X}}_k(\mathbf{p}) = (\mathbf{A}_p \otimes \mathbf{B}_p)^H \mathbf{X}_k; \quad \mathbf{p}=0,1,2,\dots,P-1 \quad (4)$$

where \mathbf{X}_k is the space-time snapshot from the k^{th} range cell and \mathbf{A}_p and \mathbf{B}_p are scheme-dependent matrices. The operations in (4) can be interpreted as a pre-processor applied to the received signals. This pre-processing generates data for the adaptive processing to follow. Note that \mathbf{P} vectors are produced by the operations in (4). Typically, the pre-processing in (4) performs a coordinate transformation and a selection operation.

We describe the adaptive processing on the \mathbf{p}^{th} vector as

$$\mathbf{y}_k(\mathbf{p}) = \mathbf{S}^H \mathbf{R}_k^{-1}(\mathbf{p}) \tilde{\mathbf{X}}_k(\mathbf{p}) / \Phi \quad (5)$$

where

$$\mathbf{R}_k(\mathbf{p}) = \frac{1}{Q} \sum_{i=k-Q/2-1, i \neq k-1, k, k+1}^{k+Q/2+1} \tilde{\mathbf{X}}_i(\mathbf{p}) \tilde{\mathbf{X}}_i(\mathbf{p})^H \quad (6)$$

and \mathbf{S} is a scheme-dependent steering vector. $\mathbf{R}_k(\mathbf{p})$ is the interference-plus-noise covariance matrix estimated from Q adjacent range cells, excluding the cell-under-test and the two closest range cells. Note that (5) resembles the SMI scheme defined in (2) and (3). Further, based on accepted principles, the

covariance matrix estimation of an $r \times r$ matrix like $\mathbf{R}_k(\mathbf{p})$ nominally requires $Q = 2r$ iid secondary data. The term Φ in the denominator of (5) is the normalization to provide CFAR in homogeneous clutter and is given by

$$\Phi = \mathbf{S}^H \mathbf{R}_k^{-1} \mathbf{S} \quad (7)$$

In different schemes, $\mathbf{y}_k(\mathbf{p})$ may or may not be the final output of interest. If $\mathbf{y}_k(\mathbf{p})$ is the final output of interest, its magnitude will be compared to a threshold to decide if signal is present. For cases where $\mathbf{y}_k(\mathbf{p})$ will be processed further, we assemble the complex outputs from each adaptive processor as

$$\tilde{\mathbf{Y}}_k = [\mathbf{y}_k(0), \mathbf{y}_k(1), \dots, \mathbf{y}_k(P-1)]^T \quad (8)$$

and compute

$$\tilde{\mathbf{Z}}_{k,m} = \mathbf{f}_m^H \tilde{\mathbf{Y}}_k \quad (9)$$

which we call post-processing (after adaptive processing). Typically, \mathbf{f}_m is the m^{th} column of a $P \times P$ filter matrix \mathbf{F} , and $\mathbf{Z}_{k,m}$ is the final output whose magnitude will be compared to a threshold to produce a decision.

2.2 ADPCA and its beamspace version

Define a set of P sub-CPIs $\mathbf{X}_k(\mathbf{p})$, $\mathbf{p}=0, \dots, P-1$ in the k^{th} snapshot. Each sub-CPI contains possible signal returns from K_s pulses and all N

elements. Fig. 1 shows two different ways to form the sub-CPIs. As indicated in Fig. 1, implementation (a) does not overlap pulses. Given M pulses in a CPI where M can be divided by K_t , implementation (a) generates $P=M/K_t$ sub-CPIs. The 0^{th} sub-CPI consists of pulses $0, \dots, K_t-1$ and the p^{th} sub-CPI consists of pulses pK_t, \dots, pK_t+K_t-1 . Implementation (b) forms the sub-CPIs by using the same pulse returns in several sub-CPIs. Given M pulses in a CPI, implementation (b) generates $P=M-K_t+1$ sub-CPIs. The 0^{th} sub-CPI consists of pulses $0, \dots, K_t-1$ and the p^{th} sub-CPI consists of pulses $p, \dots, p+K_t-1$. In Fig.1, K_t is set to 3 and in implementation (b), neighboring sub-CPIs overlap 2 pulses. Of course, other overlaps are possible.

The pre-processing we have just described can be put into the framework of (4). \mathbf{B}_p is set to \mathbf{I}_N which is an $N \times N$ identity matrix and

$$\mathbf{A}_p = \begin{bmatrix} \mathbf{0}_{p(K_t-h) \times K_t} \\ \mathbf{I}_{K_t} \\ \mathbf{0}_{(M-K_t-pK_t+ph) \times K_t} \end{bmatrix} \quad (10)$$

where the notation $\mathbf{0}_{q \times m}$ refers to an $q \times m$ matrix of zeros. h indicates the number of pulses which are overlapped. In implementation (a) h is set to be zero and in implementation (b) h is set to be K_t-1 . \mathbf{A}_p is an $M \times K_t$ selection matrix.

The adaptive processing in ADPCA is described by (5) with the steering vector

$$\mathbf{S} = \mathbf{S}_t \otimes \mathbf{S}_s \quad (11)$$

where \mathbf{S}_s is the $N \times 1$ spatial steering vector [5], \mathbf{S}_t is a $K_t \times 1$ vector, which is composed of the binomial coefficients, with each coefficient altered in sign (start with positive). As a particular example, we have

$$\mathbf{S}_t = (1, -2, 1)^T \quad (12)$$

for a three pulse case.

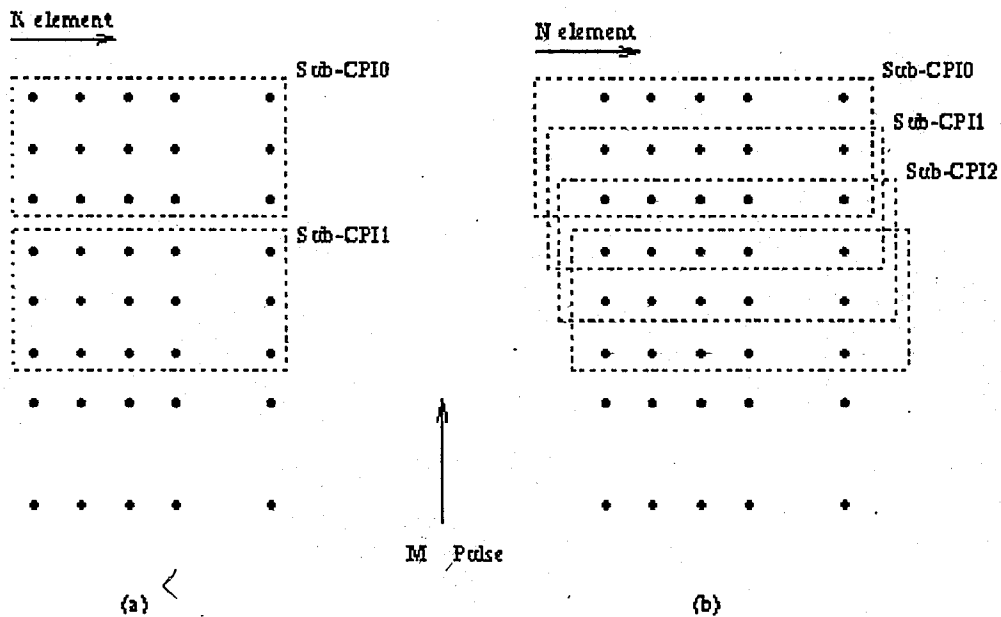


Figure 1) ADPCA sub-CPI formation

Typically, post-processing as described in (8) and (9) is employed in ADPCA. In ADPCA \mathbf{F} is a matrix corresponding to a Doppler filter bank, and \mathbf{f}_m is the filter corresponding to the m^{th} Doppler frequency. Typically \mathbf{F} is a DFT matrix

and this Doppler processing can then be efficiently implemented by computing an FFT. $\mathbf{Z}_{k,m}$, the final output for Doppler bin m , is compared to a threshold to make a decision if one is testing for a target with the Doppler frequency corresponding to this Doppler bin.

Subarraying ADPCA and beamspace ADPCA are both beamspace versions of ADPCA. \mathbf{B}_p is used as a beamformer matrix to produce $K_s \leq N$ number of beam outputs. We focus on $K_s=3$ in this thesis.

In subarraying ADPCA the beamformer matrix

$$\mathbf{B}_p = \mathbf{G} = \begin{bmatrix} \mathbf{g}_0 & \mathbf{0} & \mathbf{0} \\ \mathbf{g}_1 & \mathbf{g}_0 & \\ \vdots & \mathbf{g}_1 & \ddots \\ \mathbf{g}_{N'-1} & \vdots & \mathbf{g}_0 \\ & \mathbf{g}_{N'-1} & \ddots & \mathbf{g}_1 \\ & & & \vdots \\ \mathbf{0} & \mathbf{0} & & \mathbf{g}_{N'-1} \end{bmatrix} \quad (13)$$

is employed in (4), where $\mathbf{g} = (\mathbf{g}_0, \mathbf{g}_1, \mathbf{g}_2, \dots, \mathbf{g}_{N'-1})^T$ is a vector of scalar components and $N' = N - K_s + 1$. The vector \mathbf{g} can be any of the popular windows or tapering from the DSP [7] or radar [8] literature. Here we take \mathbf{g} as either a uniform window or the hamming window in our tests. Uniform window gave better results than hamming window so we present results for uniform \mathbf{g} vector.

Each vector produced by the pre-processing (4) will be adaptively processed as in (5) where

$$\mathbf{S} = (\mathbf{I}_{K_t} \otimes \mathbf{G})^H \mathbf{S}_e \quad (14)$$

with \mathbf{S}_e chosen as the steering vector used in adaptive processing of ADPCA .

The post processing is same as in ADPCA.

Beamspace ADPCA is identical to subarraying ADPCA but with $\mathbf{B}_p = \mathbf{G} = [\mathbf{f}_{N,1}, \mathbf{f}_{N,2}, \dots, \mathbf{f}_{N,K_s}]$, where $\mathbf{f}_{N,j}, j=1, \dots, K_s$ are those columns of $N \times N$ DFT matrix corresponding to K_s particular angle bins.

2.3 FTS and subarraying FTS

In factored post-Doppler STAP [5], Doppler processing is first performed on each spatial channel. Let the Doppler filter applied to each spatial channel be represented by \mathbf{f}_p . (a target is assumed to have the Doppler frequency corresponding to this filter). For convenience collect the Doppler filters in the $M \times M$ matrix $\mathbf{F}_M = [\mathbf{f}_0, \mathbf{f}_1, \dots, \mathbf{f}_{M-1}]$. Then the pre-processing is described by (4) with $\mathbf{A}_p = \mathbf{f}_p$, $\mathbf{P} = \mathbf{M}$, and $\mathbf{B}_p = \mathbf{I}_N$. This pre-processing transforms the signal into Doppler space. In this case a single pulse at a time is processed ($K_t = 1$) and p indicates the index of Doppler bin in question. To test for a target in only one particular Doppler bin only the calculations for a single p are necessary. Next, the adaptive processing in (5) is employed with the steering vector defined as in (11). Here $\mathbf{S} = \mathbf{S}_s$, since K_t is 1. As for most of the STAP schemes we discuss, tapering could be applied to the steering vector [5]. Post-processing

is not usually employed and $|y_k(\mathbf{p})|$ is compared to a threshold to test for a target in the \mathbf{p}^{th} Doppler bin.

Subarraying FTS is identical to FTS but with $\mathbf{B}_p = \mathbf{G}$ as described in (13). The adaptive processing is as in FTS with the steering vector defined in (14). Here \mathbf{S}_e is the steering vector that is used in the adaptive processing of FTS. Post processing is not employed.

2.4 EFA and subarraying EFA

The extended factored approach (EFA) [9] is a slight extension of the factored post-Doppler approach. In EFA, adaptive processing is applied to several adjacent Doppler bins instead of just one. Thus, the pre-processing performs both transformation and selection. In the case considered here, where the scheme adapts over 3 adjacent bins, the pre-processing can be described as in (4) with $\mathbf{A}_p = \mathbf{J}_p = [\mathbf{f}_{p-1}, \mathbf{f}_p, \mathbf{f}_{p+1}]$ and $\mathbf{B}_p = \mathbf{I}_N$.

The other quantities are set in a similar manner as for factored post-Doppler STAP but with the new \mathbf{A}_p . For example, the steering vector is obtained from

$$\mathbf{s} = (\mathbf{A}_p \otimes \mathbf{B}_p)^H \mathbf{v}(\mathbf{s}) \quad (15)$$

where $\mathbf{V}(\mathbf{S})$ is the normalized target response as used in (3). As for FTS usually only one $\mathbf{y}_k(\mathbf{p})$ is tested. By selecting \mathbf{f}_p to correspond to the target Doppler frequency under consideration, the steering vector can be defined as in (11) with $\mathbf{S}_t = [\mathbf{0}, \mathbf{1}, \mathbf{0}]^T$.

In subarraying EFA, the pre-processing is the same as with EFA but with \mathbf{B}_p set as in (13). The adaptive processing is defined as in (5) with \mathbf{S} as in (15).

2.5 Joint-domain localized approach (JDL)

In JDL [10], the pre-processor performs two dimensional transformation and selection. The data is transformed from the space-time domain into the angle-Doppler domain. This pre-processing can be described as in (4), with $\mathbf{A}_p = [\mathbf{f}_{m,1}, \mathbf{f}_{m,2}, \dots, \mathbf{f}_{m,K_t}]$, where $\mathbf{f}_{m,j} j=1, \dots, K_t$ are K_t columns of an $M \times M$ DFT matrix and with $\mathbf{B}_p = \mathbf{G} = [\mathbf{f}_{n,1}, \mathbf{f}_{n,2}, \dots, \mathbf{f}_{n,K_s}]$, where $\mathbf{f}_{n,j} j=1, \dots, K_s$ are K_s columns of $N \times N$ DFT matrix. As for FTS and EFA, only the post processing corresponding to a single \mathbf{p} must be calculated to test for a target at a particular normalized Doppler and angular frequency. In this case, only one $\mathbf{y}_k(\mathbf{p})$ is tested.

If we focus on $K_t = K_s = 3$ and consider the case where the target to be detected has the Doppler frequency corresponding to $\mathbf{f}_{m,2}$ and the spatial frequency corresponding to $\mathbf{f}_{n,2}$, then the adaptive processing is performed as

described in (5) with

$$\mathbf{S} = [\mathbf{0} \ 1 \ \mathbf{0}] \otimes [\mathbf{0} \ 1 \ \mathbf{0}] \quad (16)$$

More precisely, the steering vector has all its entries equal to zero except for the one corresponding to the spatial and Doppler frequency of the target. Since only a single adaptive processing is performed, no post-processing is employed for JDL.

Chapter 3

Real Data Performance

To test the STAP algorithms described in section 2, we use data that comes from the Multi-Channel Airborne Radar Measurements (MCARM) database flight 5 acquisition 575. See [6] and [11] for detailed information about the MCARM program and the data. For each experiment, a single target signal with amplitude 0.05, a particular normalized Doppler frequency and a particular normalized spatial frequency was inserted in a particular range bin. Reference data are selected from consecutive range cells on each side of the cell-under-test, excluding the cell-under-test and the two closest cells. We employ normalized test statistics as in (5), which provide a constant false alarm rate (CFAR) characteristic for homogenous clutter [12]. The parameters used in each of the STAP algorithms studied are given in the Appendix.

For each example, we provide plots of the magnitude of the normalized test statistics for a set of range bins including the target range. We judge a scheme by how large the test statistic is at the target range in comparison to other ranges.

In the first example, we inserted a target at range bin 150 for the cases shown in Table 1. The location of the targets and an estimate of the

clutter (plus noise) power spectral density (psd) are illustrated in Fig. 2. As visible from Fig. 2, the psd estimate used is rather crude and is provided to give a rough description of the clutter environment. In the estimate no neighboring range cells are averaged and blackman windowing is used. Some of the artifacts can be removed by averaging, but this was not considered necessary in this case.

Case	Normalized Doppler Frequency	Normalized Spatial Frequency
a	-0.2656	-0.2656
b	-0.0312	-0.0312
c	0.125	0.203
d	-0.0312	-0.1875
e	-0.0312	0.203
f	0.3593	-0.1875
g	-0.1875	0.3593

Table 1) Test cases for each example.

A summary of the results is given in Table 2. Fig. 3 through Fig. 9 present the results for most of the schemes tested. FTS and subarraying FTS generally perform poorly, so their results are not shown. In this example, generally JDL provides best results. JDL is best in every case except cases d and e. In case d, BeamAD slightly outperforms JDL and ADPCA, but the

difference is quite small. In case e, EFA outperforms the others, however JDL also performs well. The apparently large interference near a normalized Doppler frequency of -0.0312 indicated by Fig.2 could be the reason why JDL is not best in these two cases. These are apparently difficult cases where no scheme can really excel. Table 2 shows that case b is also quite difficult, but here JDL performs much better than the other schemes. The extra clutter ridges in Fig. 2 are discussed in [13], and [14].

In the second example, we inserted a target at range bin 350. We present results for the same cases in Table 1. The best three schemes for all the cases are given in Table 3. The location of the targets and an estimate of the clutter psd is given in Fig. 10. The normalized test statistics for the six best schemes tested for each case in Table 1 are given in Figures 11 through 17. The results indicate that none of the schemes always outperforms all the others. However post-Doppler algorithms are generally better than pre-Doppler algorithms. Either JDL or EFA were best in all but case b. In case b, where the target is inserted in the largest clutter of all cases, BEFA is only slightly better than EFA and JDL.

Next, we inserted a target at range bin 415. We present results for the same cases as in previous examples. The location of the targets and an estimate of the clutter psd is given in Fig. 18. A summary of the results is in Table 4. Here for cases b, c, d, f, and g either JDL, or BEFA provide best performance. In the other cases, EFA is best and JDL also performs well. JDL

performs well in every case except case b. Even in this case, its performance is not bad. EFA and its beamspace version are best in some cases and near-best in others. ADPCA and its beamspace version give good performance in number of cases, but these schemes were never best in this example.

Finally, we test the same cases as before when the target is inserted in range bin 500. The locations of the targets and an estimate of the clutter psd is given in Fig. 19. A summary of the results is given in Table 5. Again JDL, EFA and BEFA outperform the other algorithms except for case e where ADPCA is best.

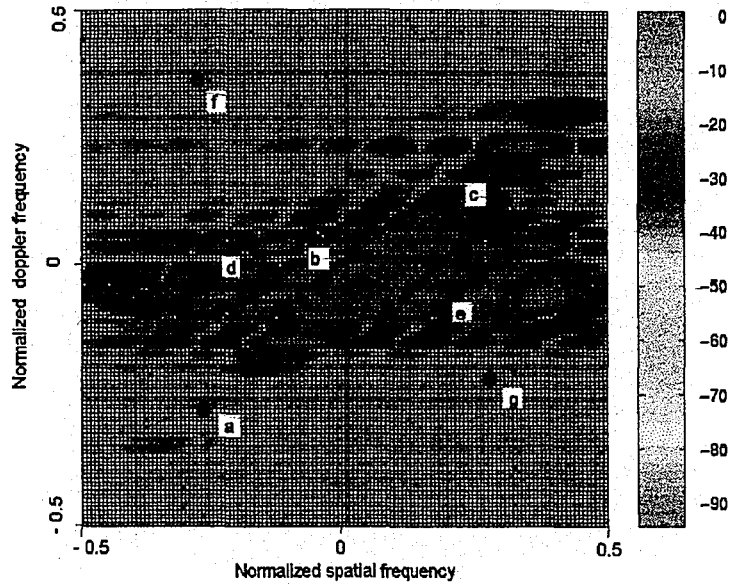


Figure 2) Power spectrum plot of range 150

Case	Normalized Doppler Frequency	Normalized Spatial Frequency	The 3 best schemes	D	Figure
a	-0.2656	-0.2656	JDL BEFA BeamAD	36 25 16	3
b	-0.0312	-0.0312	JDL	10	4
c	0.125	0.203	JDL EFA	30 12	5
d	-0.0312	-0.1875	BeamAD JDL ADPCA	8 7 6	6
e	-0.0312	0.203	EFA JDL BeamAD	20 12 5	7
f	0.3593	-0.1875	JDL EFA BeamAD	43 38 30	8
g	-0.1875	0.3593	JDL BEFA BeamAD	38 18 7	9

Table 2) The three best schemes for all the cases when the target is inserted at range 150. (D is the approximate difference between the normalized test statistic at the target and the largest peak in the normalized test statistic at some other range)

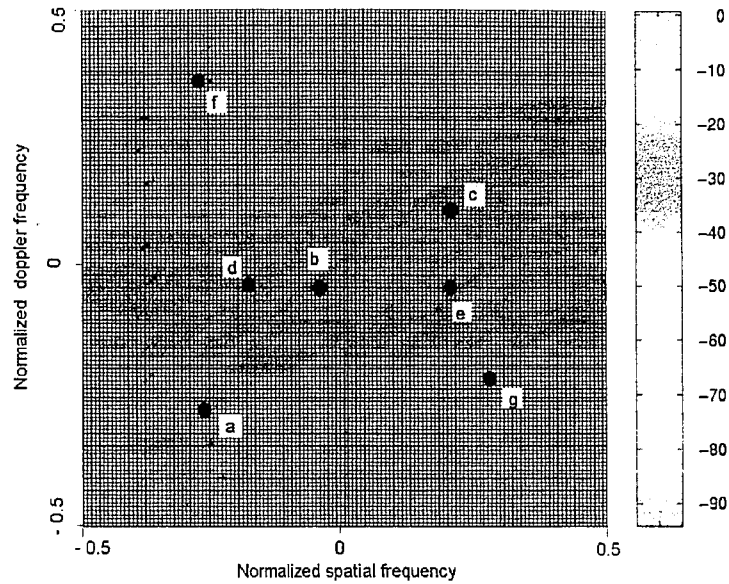
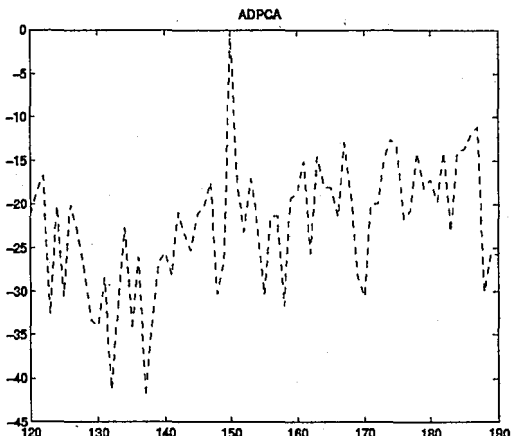


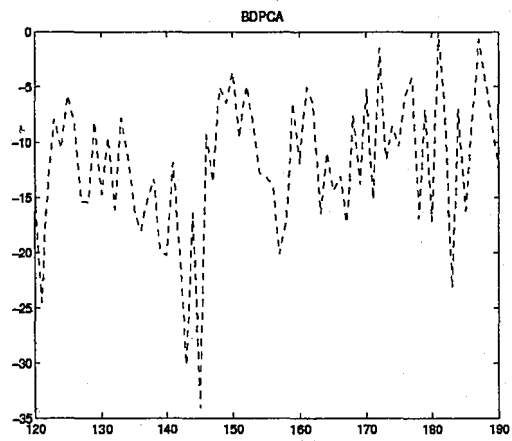
Figure 2) Power spectrum plot of range 150

Case	Normalized Doppler Frequency	Normalized Spatial Frequency	The 3 best schemes	D	Figure
a	-0.2656	-0.2656	JDL BEFA BeamAD	36 25 16	3
b	-0.0312	-0.0312	JDL	10	4
c	0.125	0.203	JDL EFA	30 12	5
d	-0.0312	-0.1875	BeamAD JDL ADPCA	8 7 6	6
e	-0.0312	0.203	EFA JDL BeamAD	20 12 5	7
f	0.3593	-0.1875	JDL EFA BeamAD	43 38 30	8
g	-0.1875	0.3593	JDL BEFA BeamAD	38 18 7	9

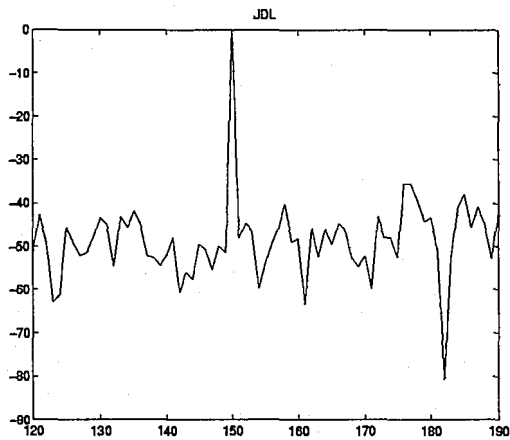
Table 2) The three best schemes for all the cases when the target is inserted at range 150. (D is the approximate difference between the normalized test statistic at the target and the largest peak in the normalized test statistic at some other range)



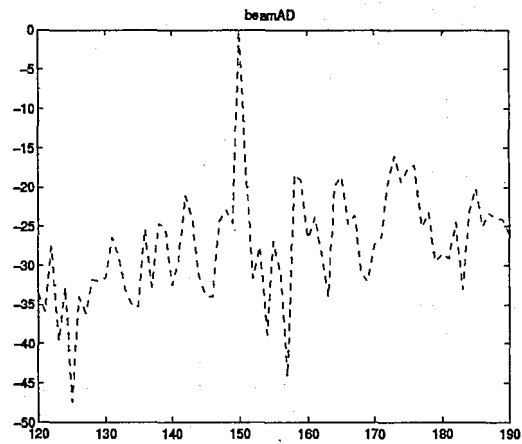
a) ADPCA



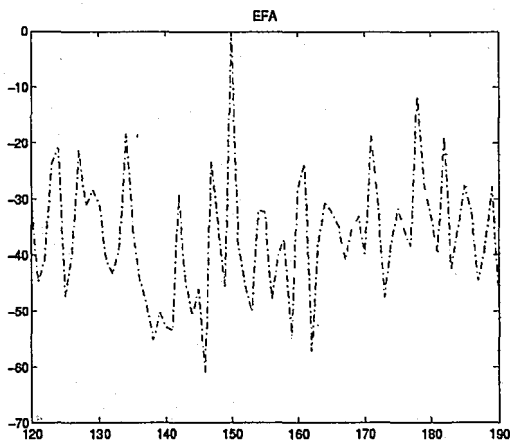
b) BDPCA



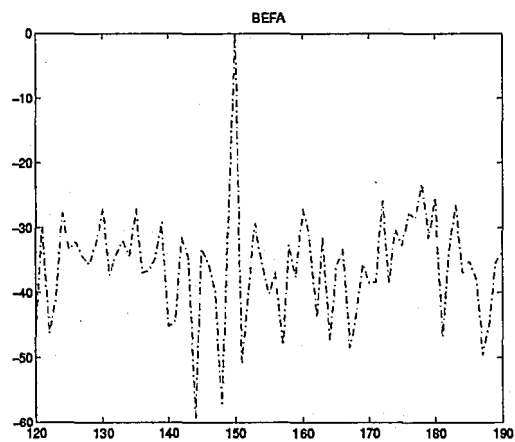
c) JDL



d) BeamAD

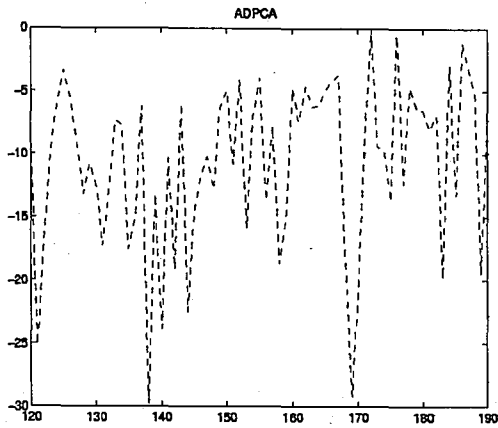


e) EFA

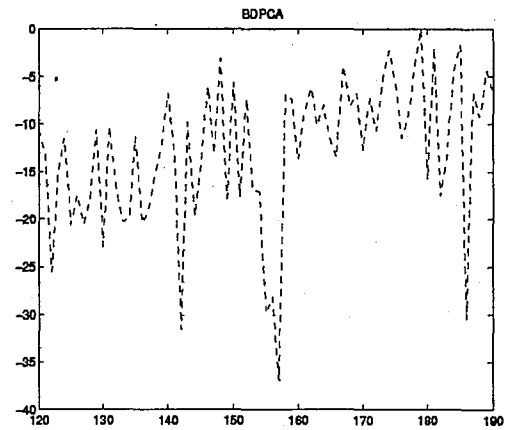


f) BEFA

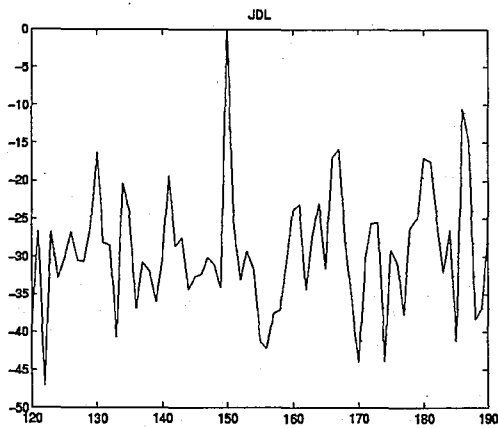
Figure 3) Performance comparison when target is inserted at range 150, case a.



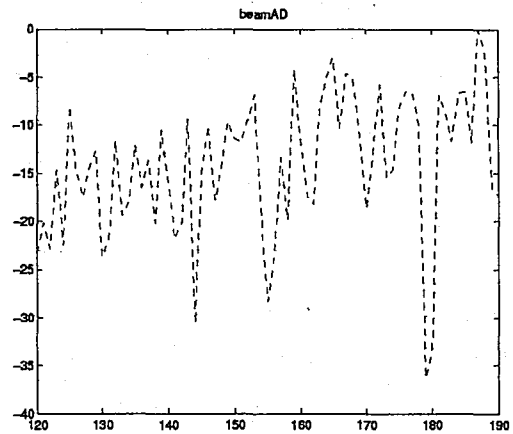
a) ADPCA



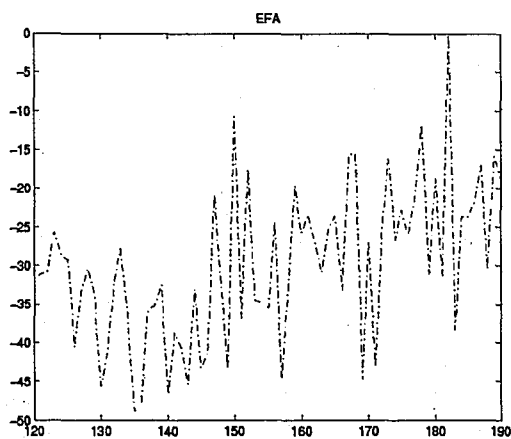
b) BDPCA



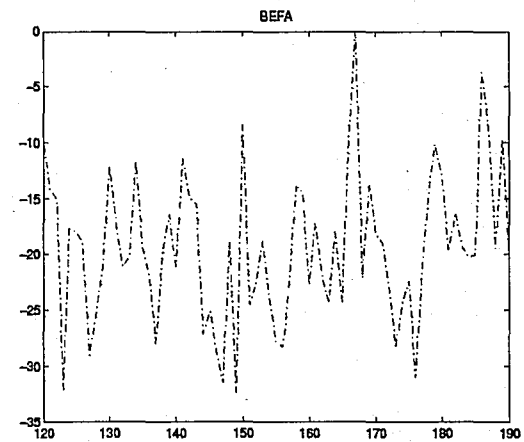
c) JDL



d) BeamAD

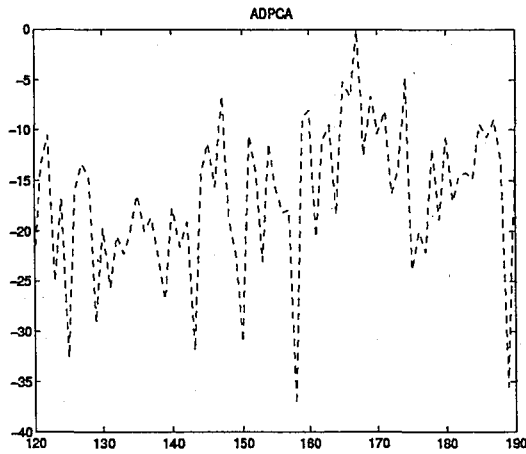


e) EFA

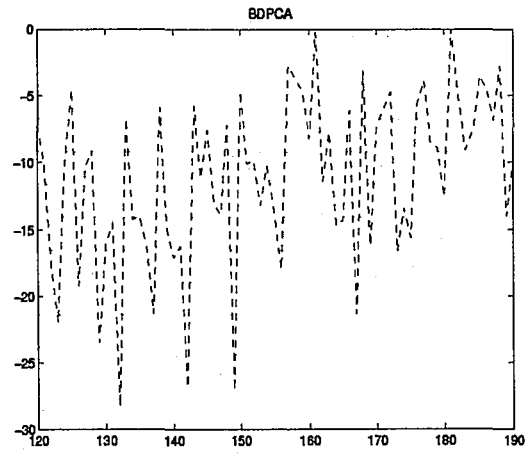


f) BEFA

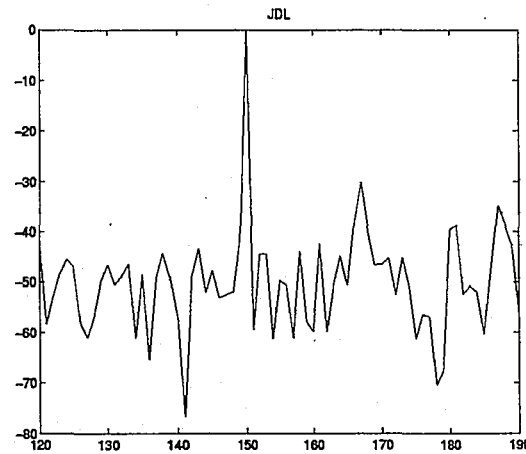
Figure 4) Performance comparison when target is inserted at range 150, case b.



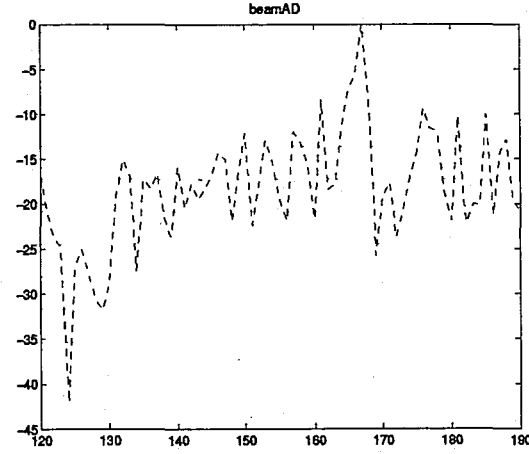
a) ADPCA



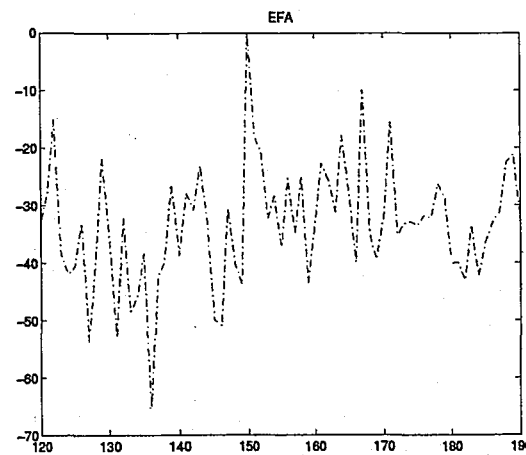
b) BDPCA



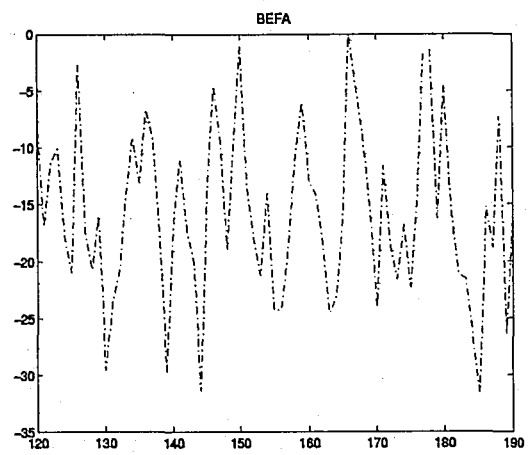
c) JDL



d) BeamAD

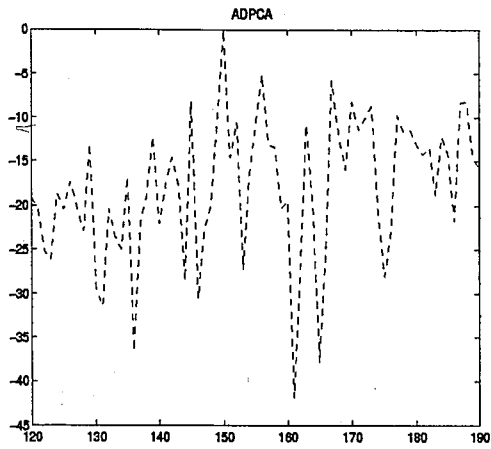


e) EFA

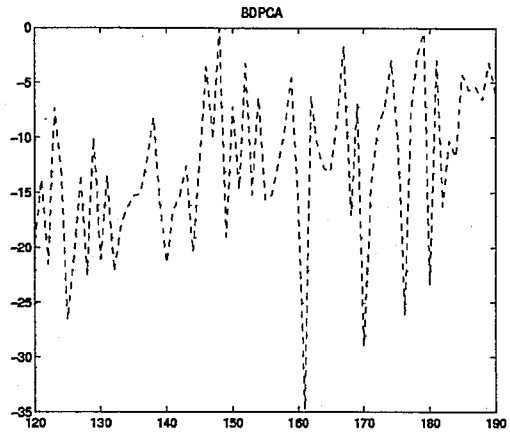


f) BEFA

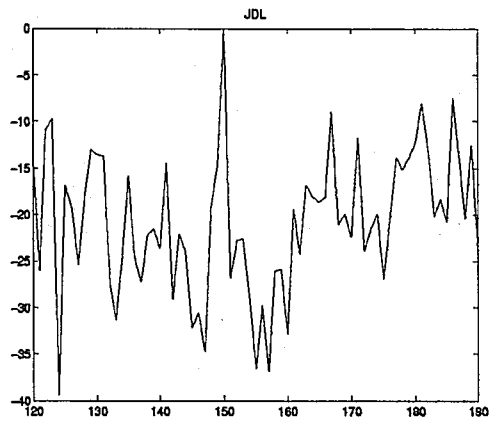
Figure 5) Performance comparison when target is inserted at range 150, case c.



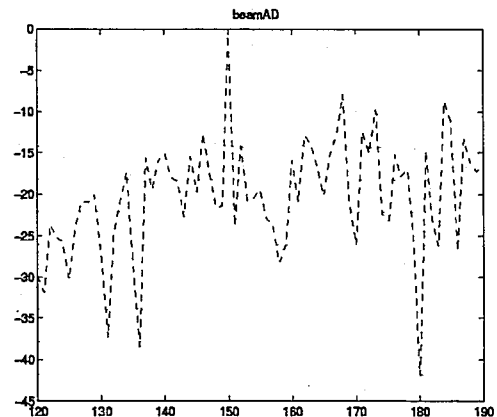
a) ADPCA



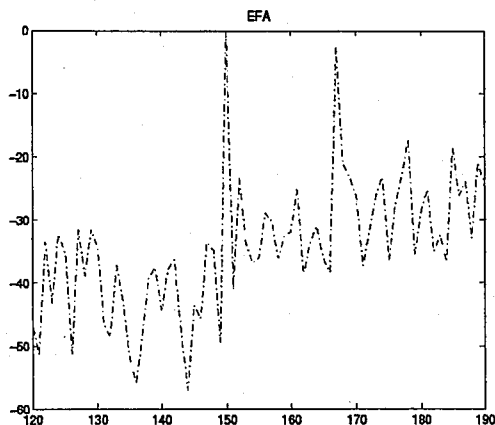
b) BDPCA



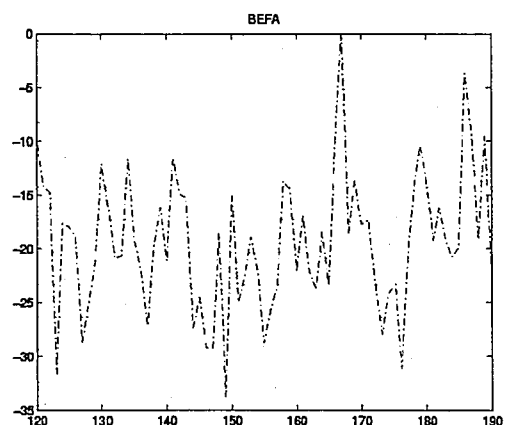
c) JDL



d) BeamAD

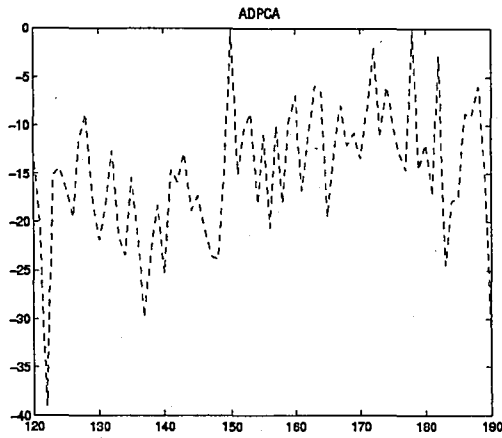


e) EFA

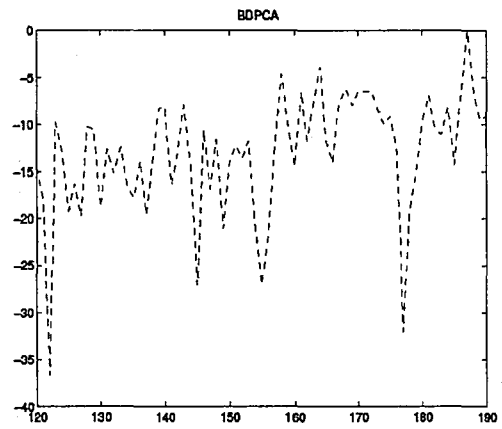


f) BEFA

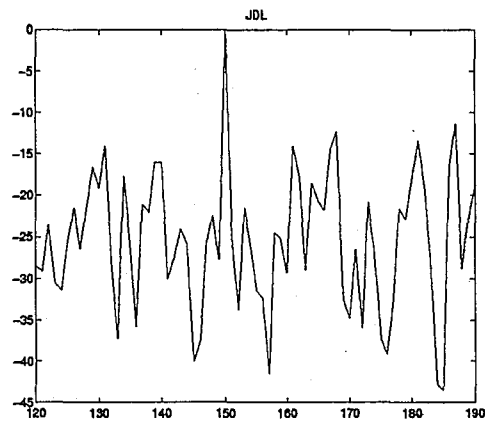
Figure 6) Performance comparison when target is inserted at range 150, case d.



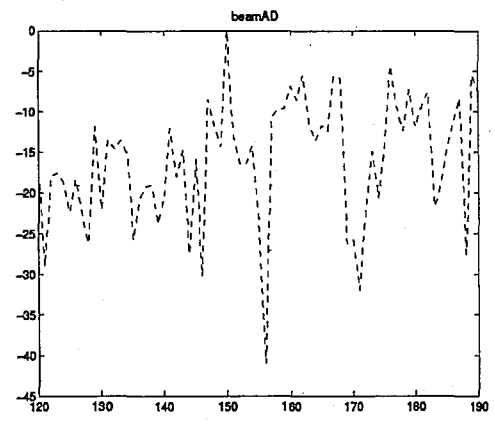
a) ADPCA



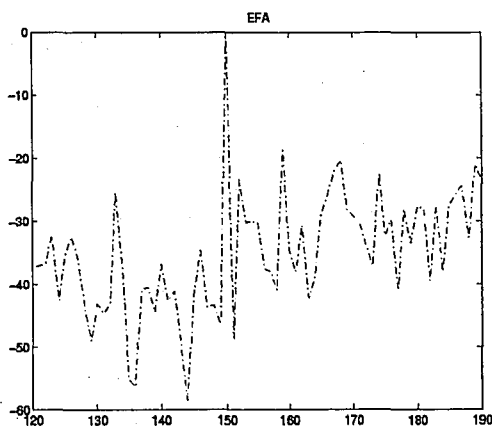
b) BDPCA



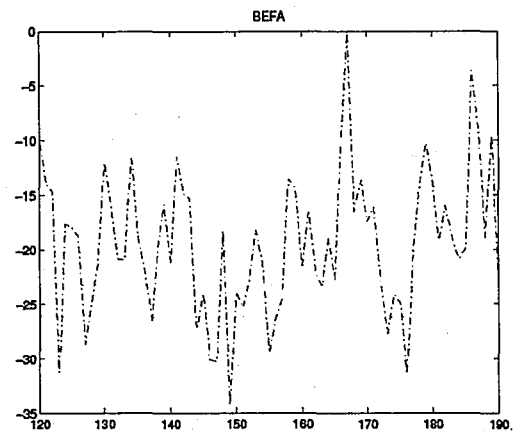
c) JDL



d) BeamAD

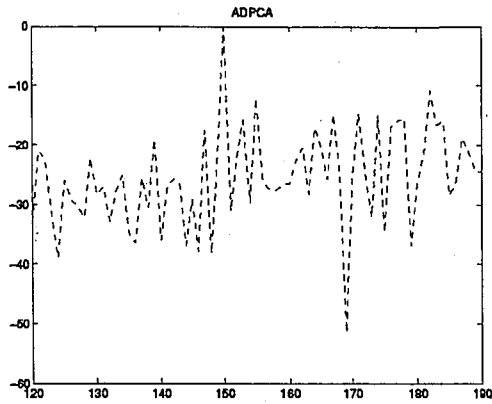


e) EFA

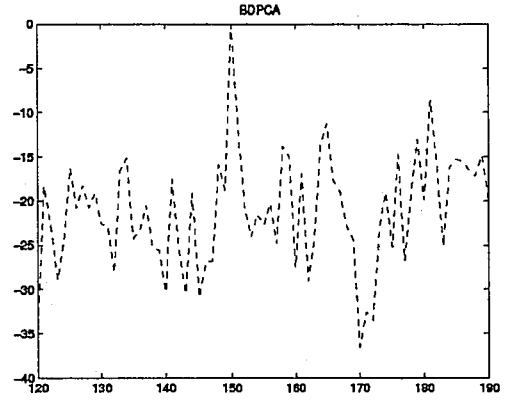


f) BEFA

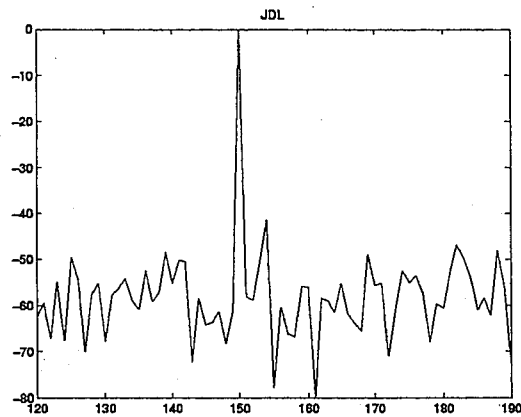
Figure 7) Performance comparison when target is inserted at range 150, case e.



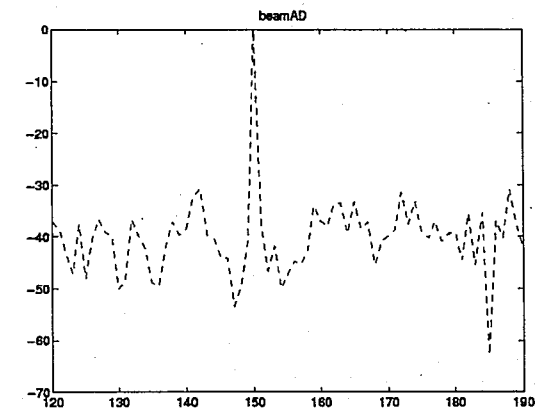
a) ADPCA



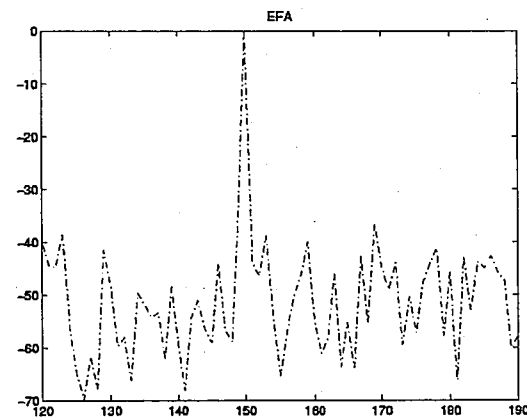
b) BDPCA



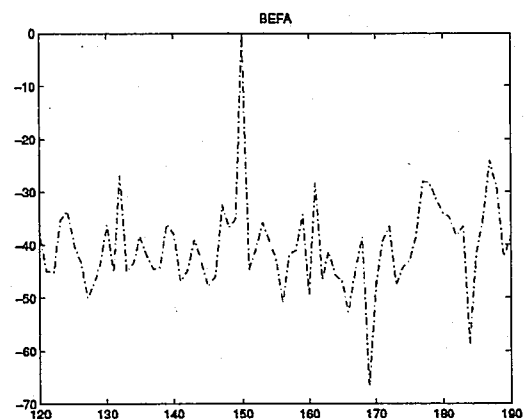
c) JDL



d) BeamAD

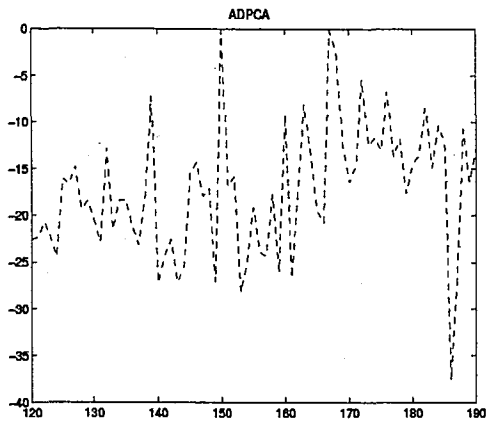


e) EFA

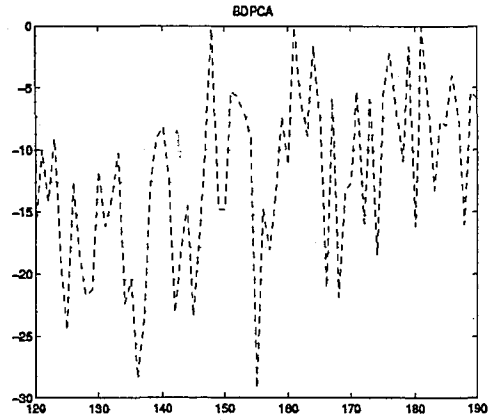


f) BEFA

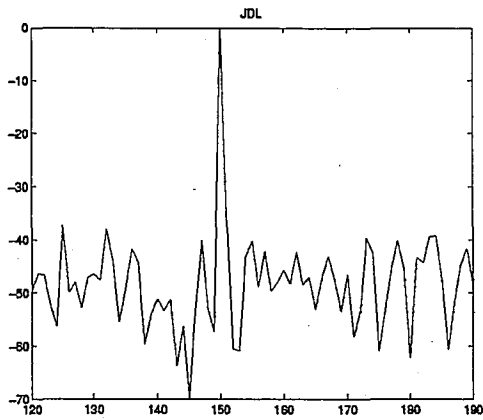
Figure 8) Performance comparison when target is inserted at range 150, case f.



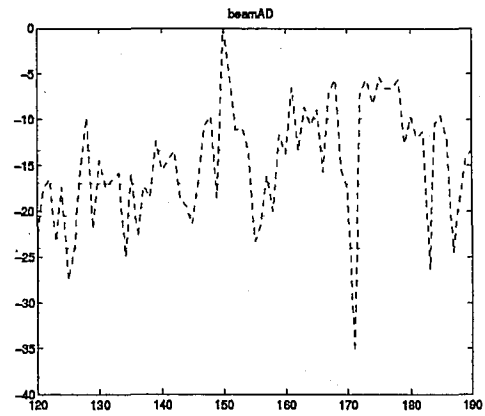
a) ADPCA



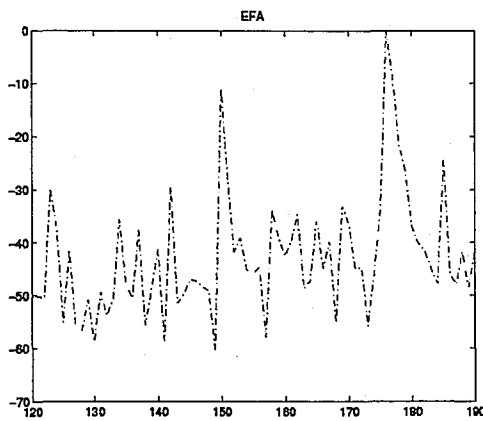
b) BDPCA



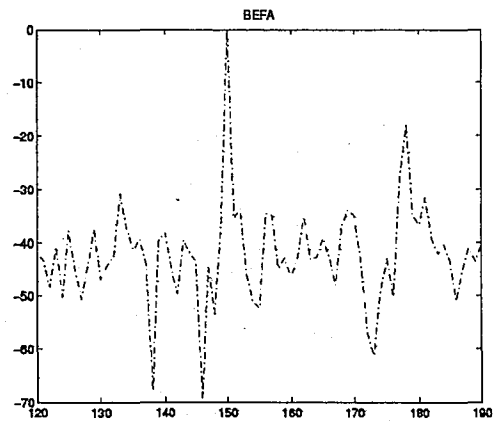
c) JDL



d) BeamAD



e) EFA



f) BEFA

Figure 9) Performance comparison when target is inserted at range 150, case g.

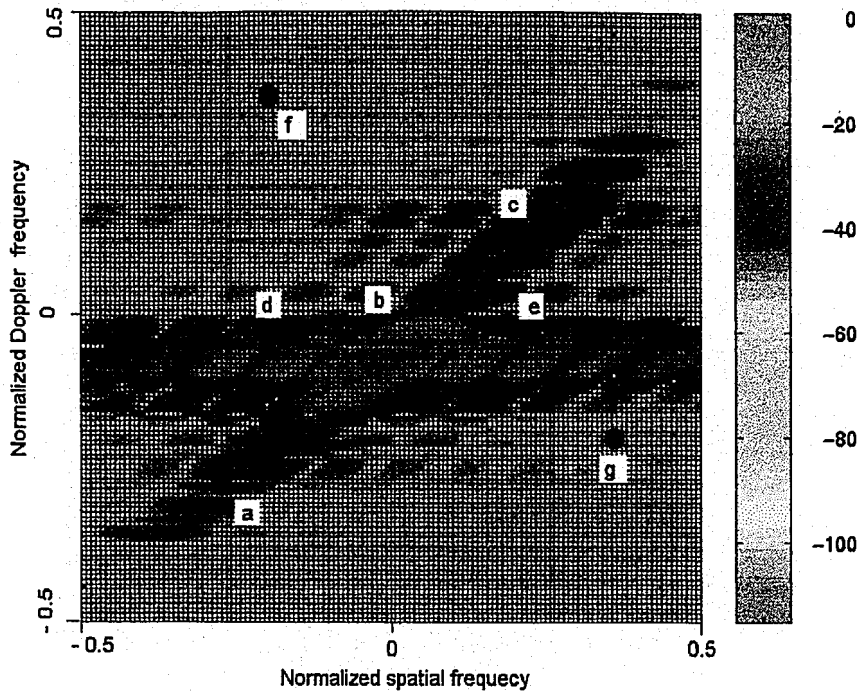


Figure 10) Power spectrum plot of range 350.

Case	Normalized Doppler Frequency	Normalized Spatial Frequency	The 3 best schemes	D	Figure
a	-0.2656	-0.2656	EFA JDL BEFA	24 18 5	11
b	-0.0312	-0.0312	BEFA EFA JDL	15 12 10	12
c	0.125	0.203	JDL EFA BEFA	34 25 13	13
d	-0.0312	-0.1875	EFA JDL ADPCA	28 20 12	14
e	-0.0312	0.203	EFA JDL ADPCA	22 18 7	15
f	0.3593	-0.1875	EFA JDL BeamAD	48 43 24	16
g	-0.1875	0.3593	JDL BEFA BeamAD	33 18 14	17

Table 3) The three best schemes for all the cases when the target is inserted at range 350. (D is the approximate difference between the normalized test statistic at the target and the largest peak in the normalized test statistic at some other range.)

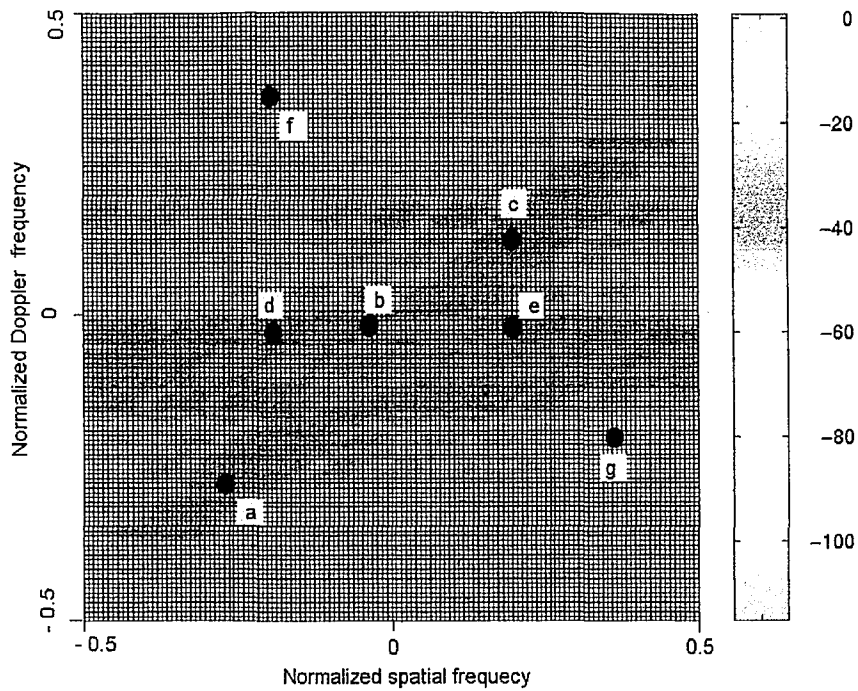
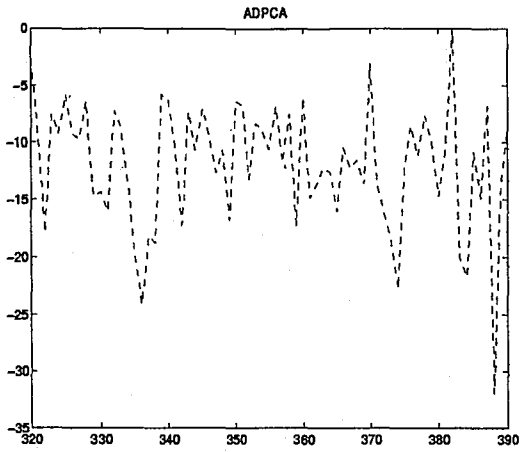


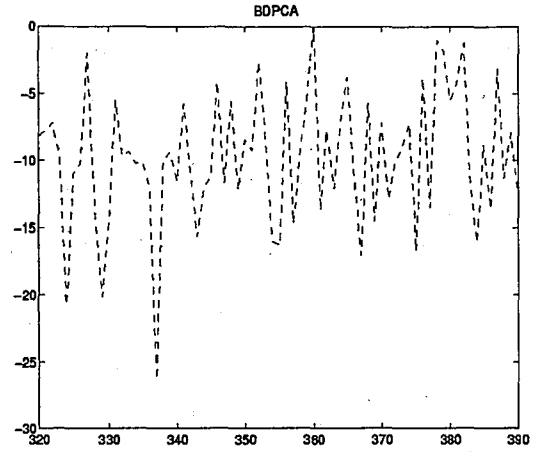
Figure 10) Power spectrum plot of range 350.

Case	Normalized Doppler Frequency	Normalized Spatial Frequency	The 3 best schemes	D	Figure
a	-0.2656	-0.2656	EFA JDL BEFA	24 18 5	11
b	-0.0312	-0.0312	BEFA EFA JDL	15 12 10	12
c	0.125	0.203	JDL EFA BEFA	34 25 13	13
d	-0.0312	-0.1875	EFA JDL ADPCA	28 20 12	14
e	-0.0312	0.203	EFA JDL ADPCA	22 18 7	15
f	0.3593	-0.1875	EFA JDL BeamAD	48 43 24	16
g	-0.1875	0.3593	JDL BEFA BeamAD	33 18 14	17

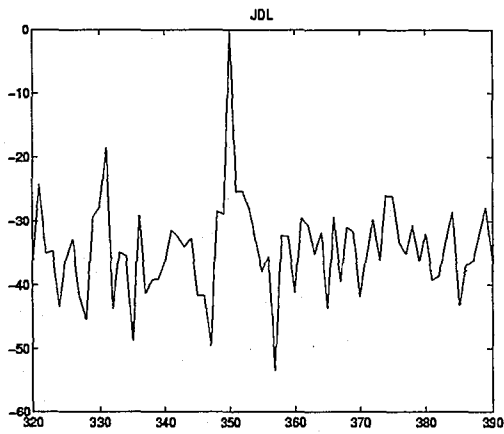
Table 3) The three best schemes for all the cases when the target is inserted at range 350. (D is the approximate difference between the normalized test statistic at the target and the largest peak in the normalized test statistic at some other range.)



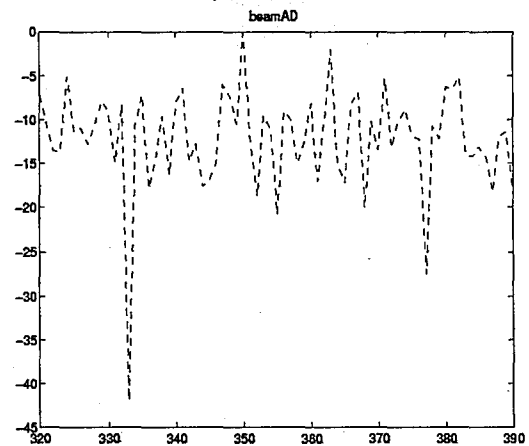
a) ADPCA



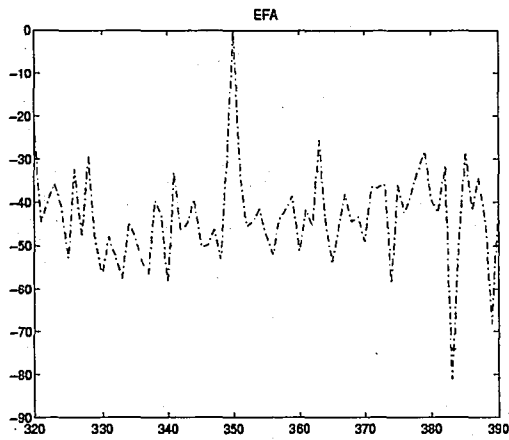
b) BDPCA



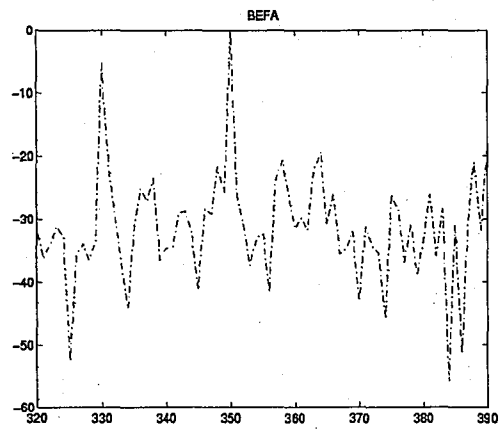
c) JDL



d) BeamAD

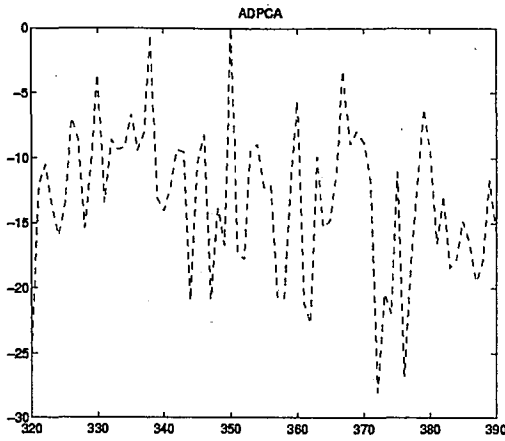


e) EFA

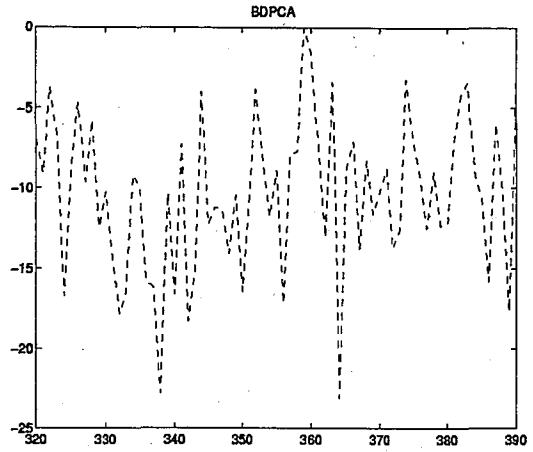


f) BEFA

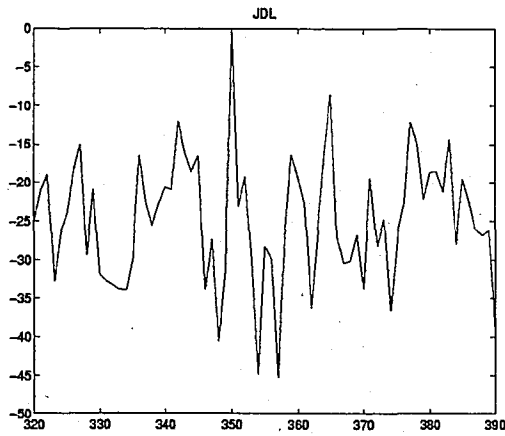
Figure 11) Performance comparison when target is inserted at range 350, case a.



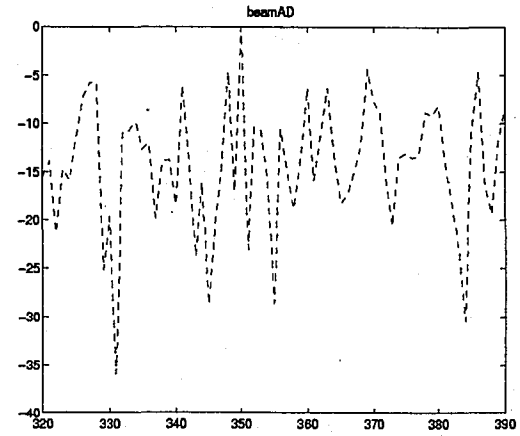
a) ADPCA



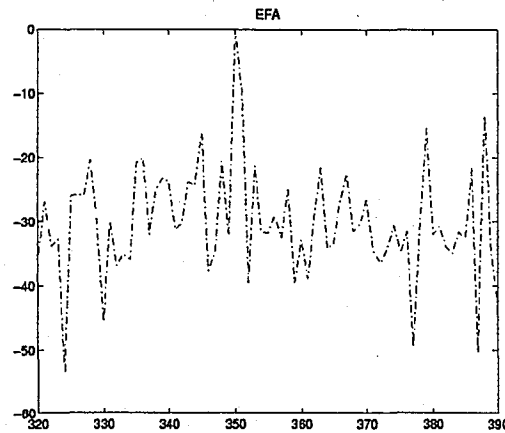
b) BDPCA



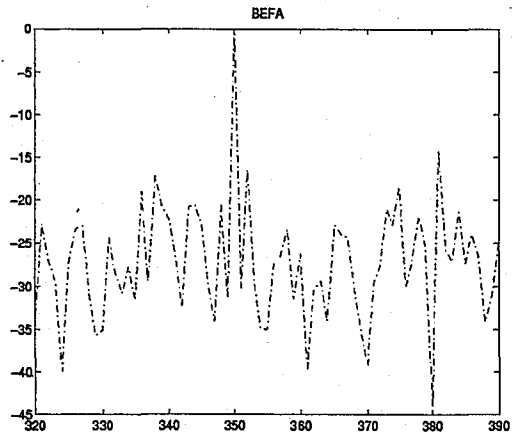
c) JDL



d) BeamAD

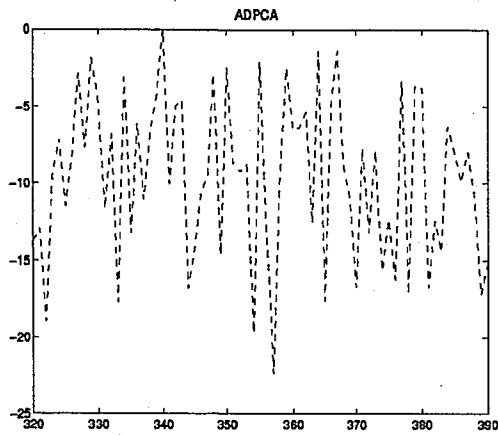


e) EFA

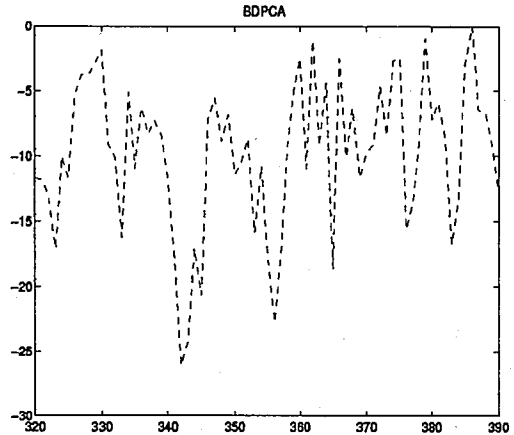


f) BEFA

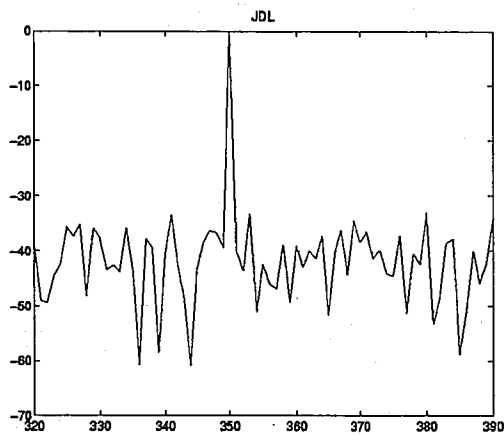
Figure 12) Performance comparison when target is inserted at range 350, case b.



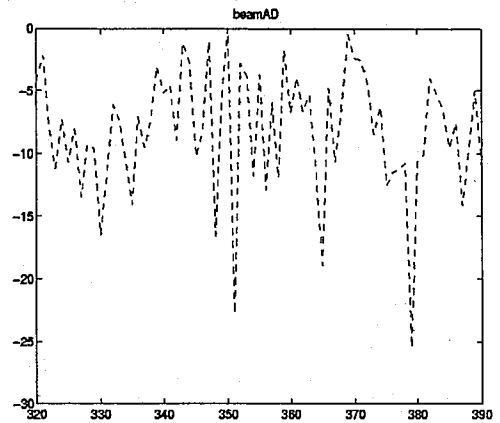
a) ADPCA



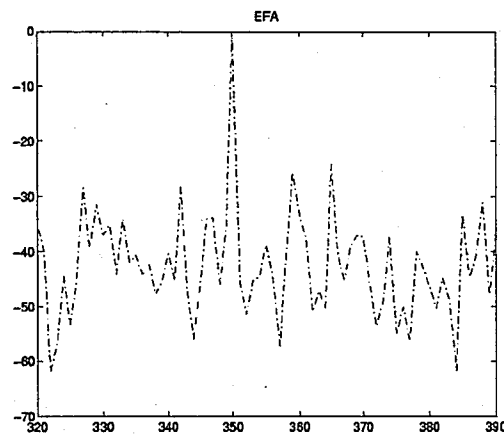
b) BDPCA



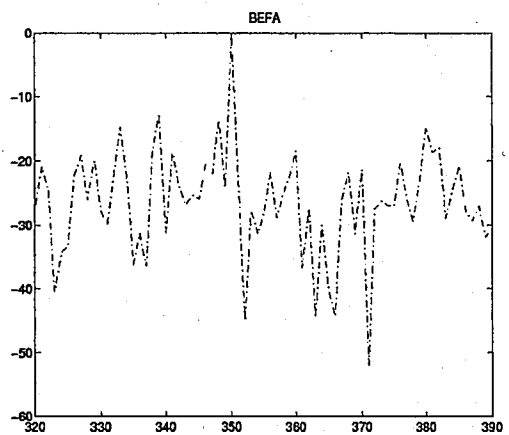
c) JDL



d) BeamAD

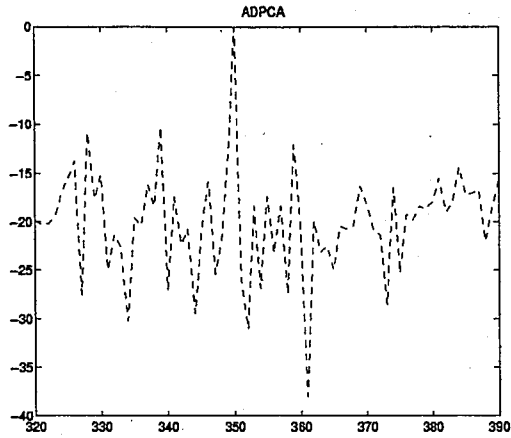


e) EFA

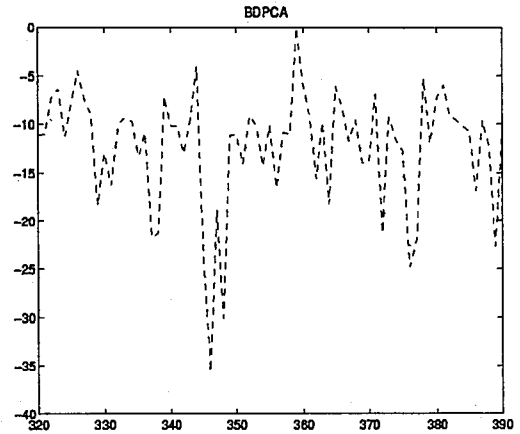


f) BEFA

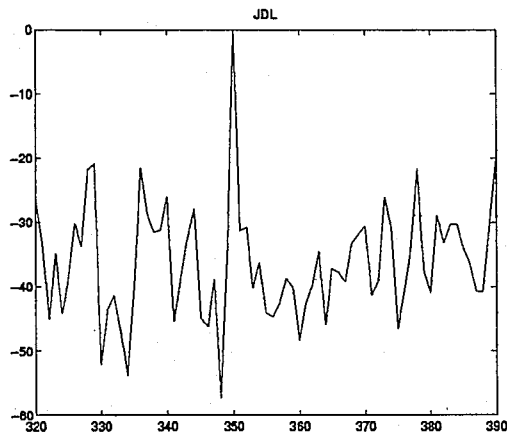
Figure 13) Performance comparison when target is inserted at range 350, case c.



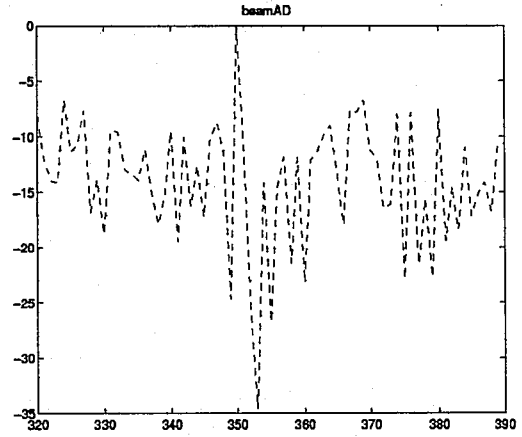
a) ADPCA



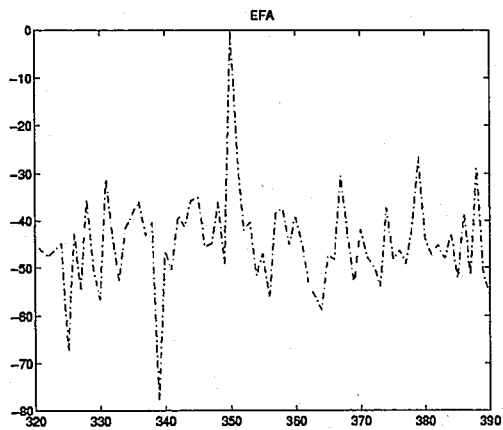
b) BDPCA



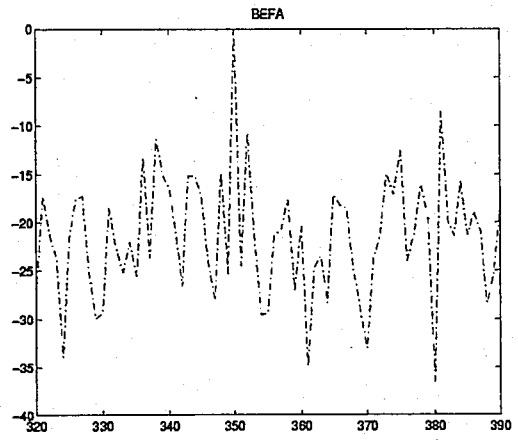
c) JDL



d) BeamAD

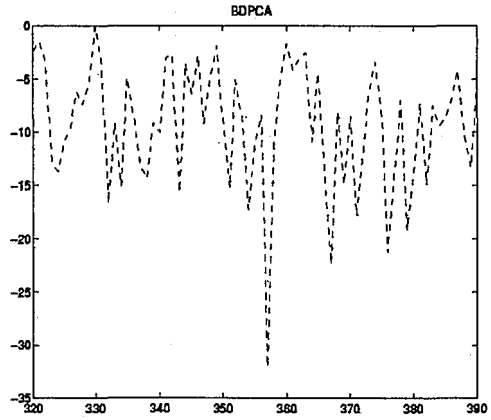
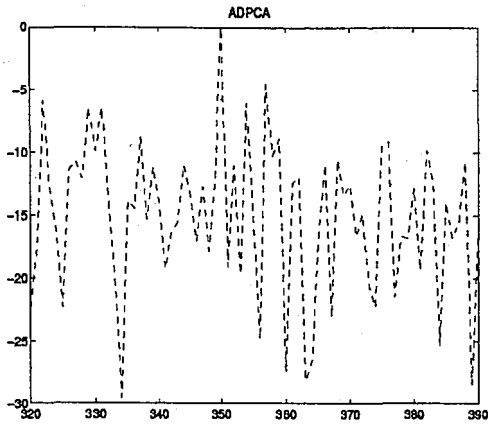


e) EFA



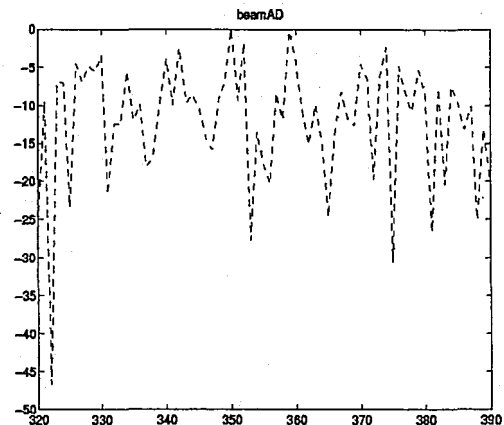
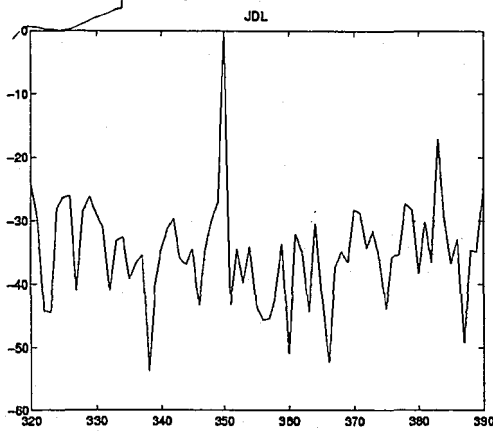
f) BEFA

Figure 14) Performance comparison when target is inserted at range 350, case d.



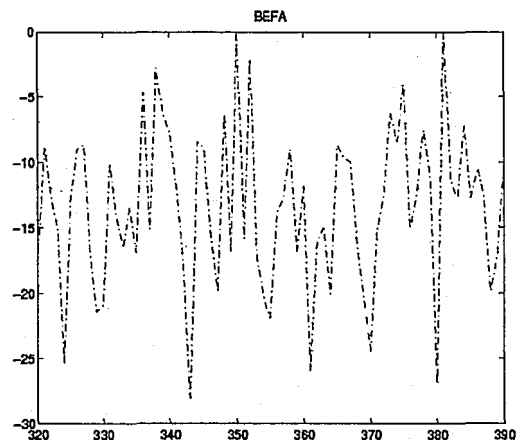
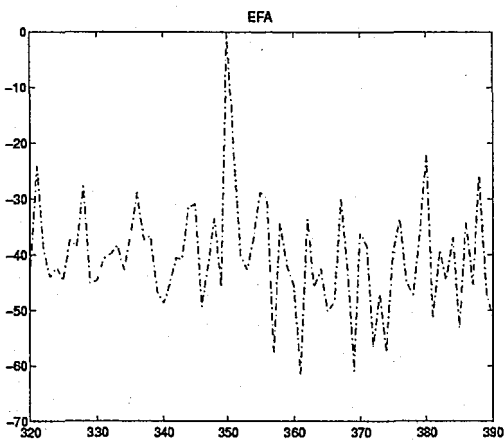
a) ADPCA

b) BDPCA



c) JDL

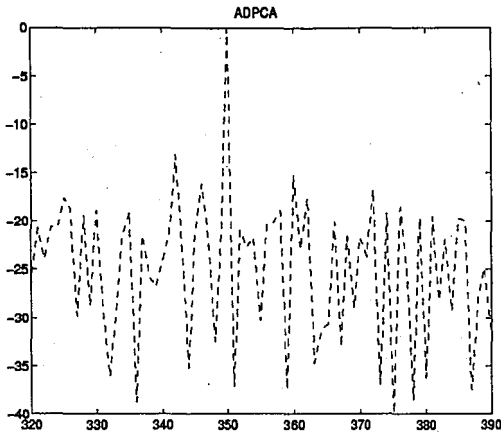
d) BeamAD



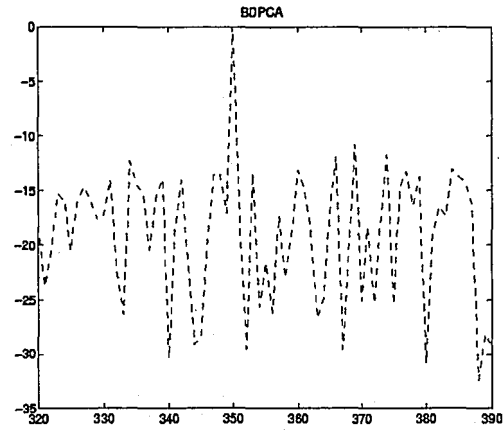
e) EFA

f) BEFA

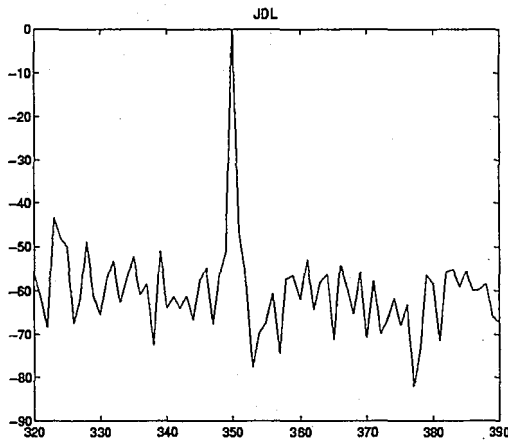
Figure 15) Performance comparison when target is inserted at range 350, case e.



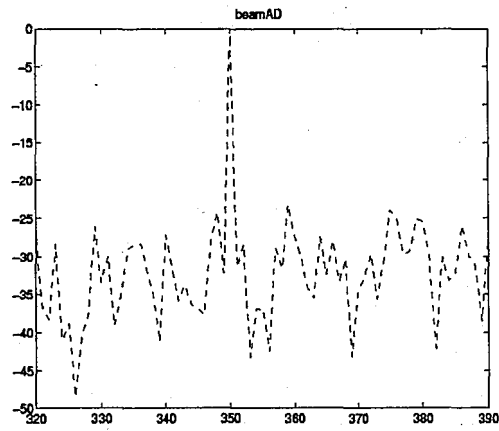
a) ADPCA



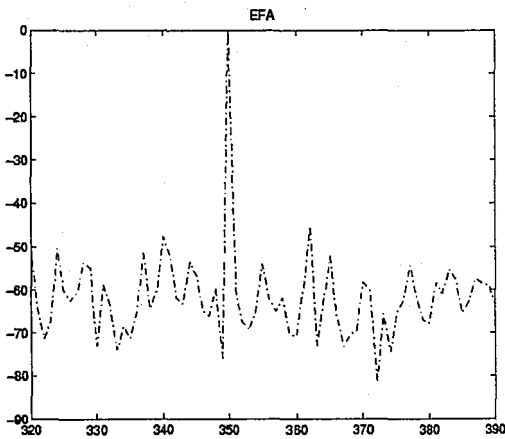
b) BDPCA



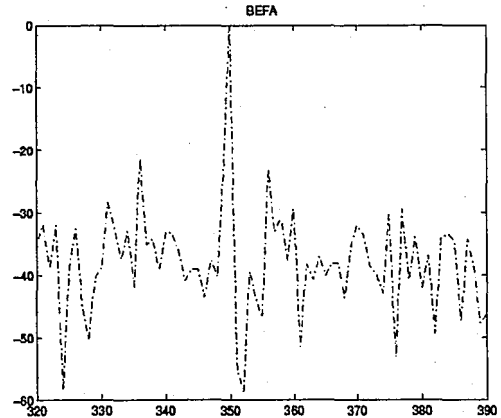
c) JDL



d) BeamAD

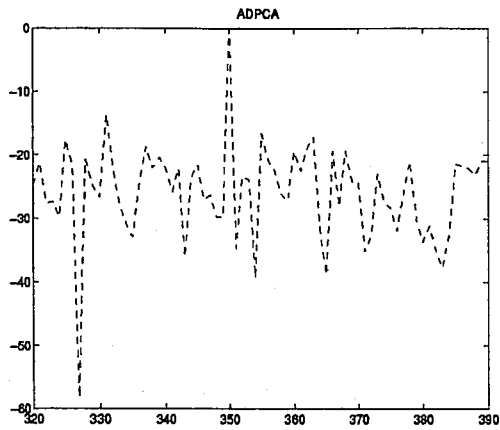


e) EFA

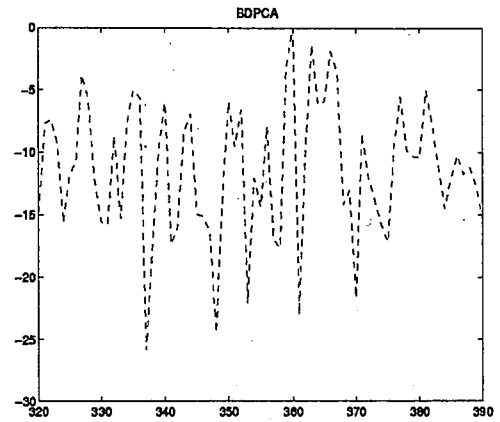


f) BEFA

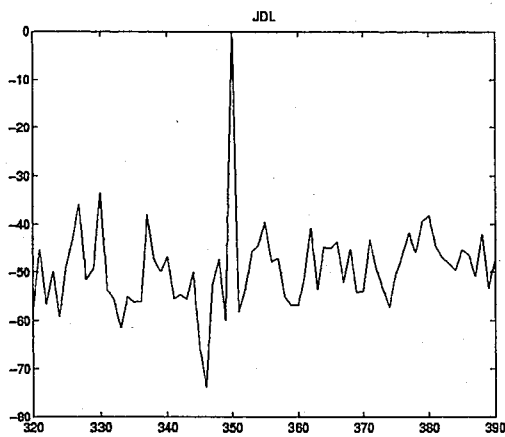
Figure 16) Performance comparison when target is inserted at range 350, case f.



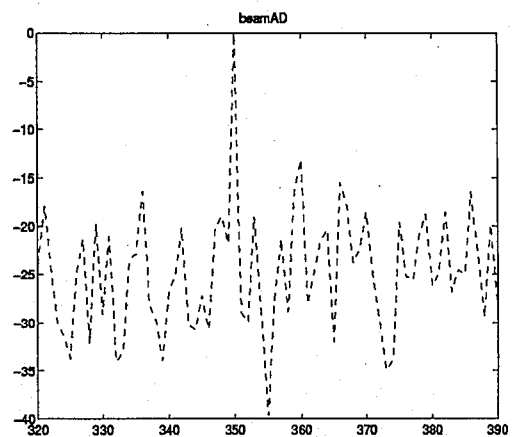
a) ADPCA



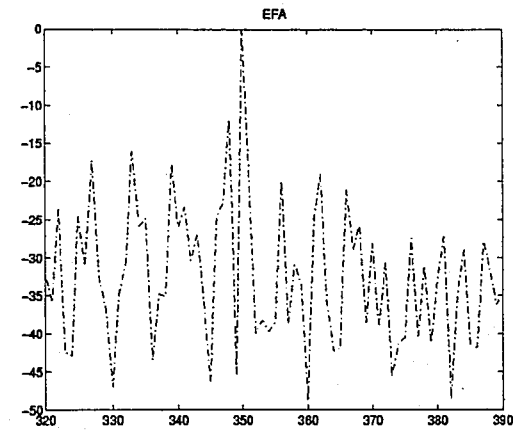
b) BDPCA



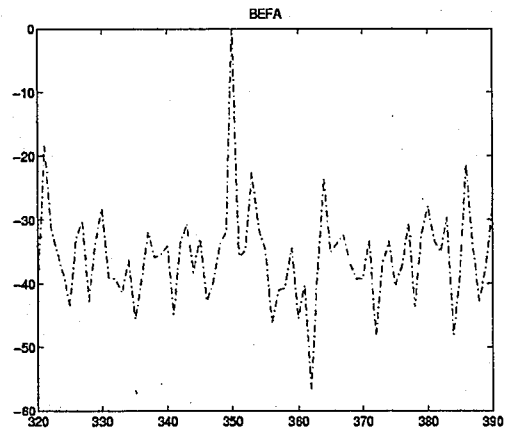
c) JDL



d) BeamAD



e) EFA



f) BEFA

Figure17) Performance comparison when target is inserted at range 350, case g.

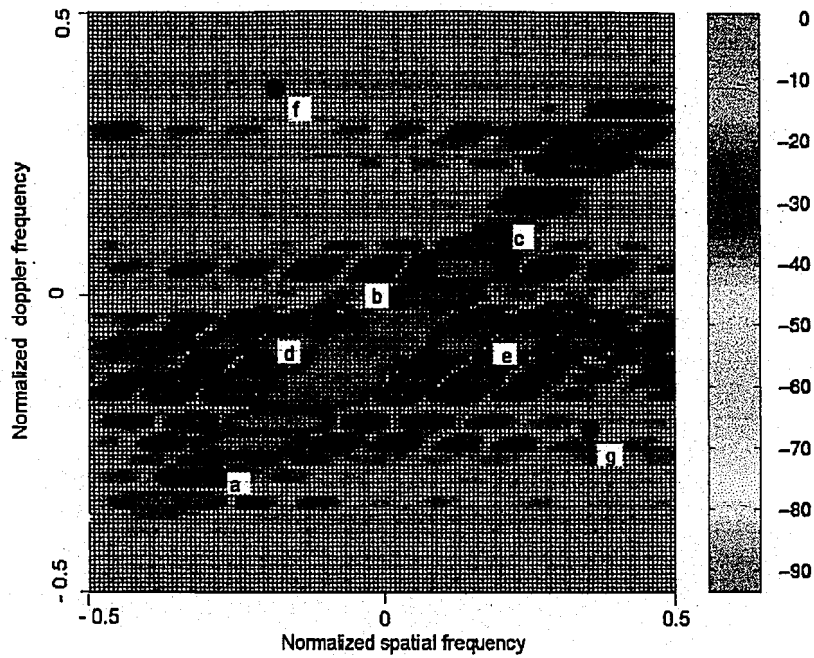


Figure 18) Power spectrum plot of range 415

Case	Normalized Doppler Frequency	Normalized Spatial Frequency	The 3 best schemes	D
a	-0.2656	-0.2656	EFA JDL ADPCA	25 22 12
b	-0.0312	-0.0312	BEFA BeamAD EFA, ADPCA	25 18 15
c	0.125	0.203	BEFA JDL BeamAD	30 23 12
d	-0.0312	-0.1875	JDL, BEFA BeamAD EFA, ADPCA	20 18 16
e	-0.0312	0.203	EFA JDL ADPCA	28 24 15
f	0.3593	-0.1875	JDL BeamAD BEFA	45 35 32
g	-0.1875	0.3593	JDL EFA BeamAD	42 20 18

Table 4) The three best schemes for all the cases when the target is inserted at range 415. (D is the approximate difference between the normalized test statistic at the target and the largest peak in the normalized test statistic at some other range)

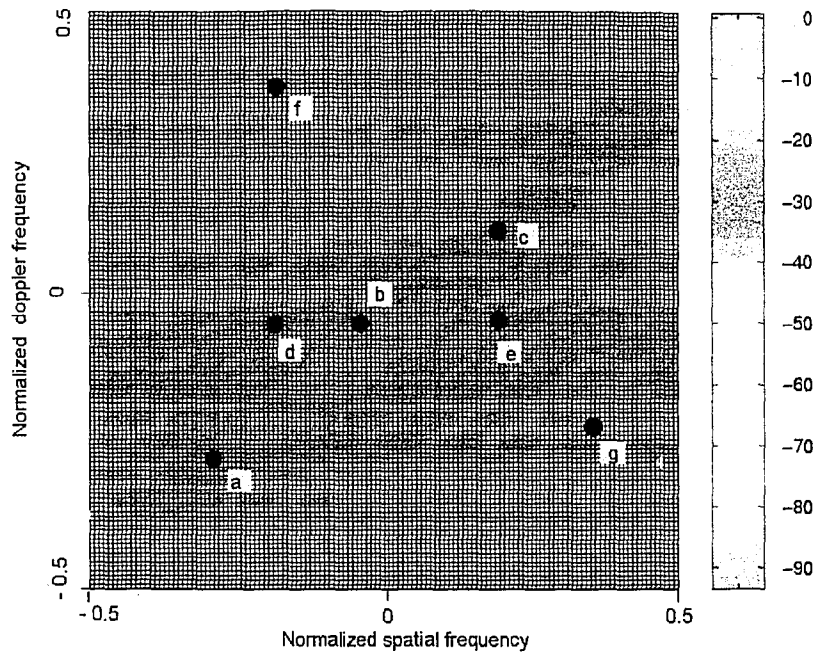


Figure 18) Power spectrum plot of range 415

Case	Normalized Doppler Frequency	Normalized Spatial Frequency	The 3 best schemes	D
a	-0.2656	-0.2656	EFA JDL ADPCA	25 22 12
b	-0.0312	-0.0312	BEFA BeamAD EFA, ADPCA	25 18 15
c	0.125	0.203	BEFA JDL BeamAD	30 23 12
d	-0.0312	-0.1875	JDL, BEFA BeamAD EFA, ADPCA	20 18 16
e	-0.0312	0.203	EFA JDL ADPCA	28 24 15
f	0.3593	-0.1875	JDL BeamAD BEFA	45 35 32
g	-0.1875	0.3593	JDL EFA BeamAD	42 20 18

Table 4) The three best schemes for all the cases when the target is inserted at range 415. (D is the approximate difference between the normalized test statistic at the target and the largest peak in the normalized test statistic at some other range)

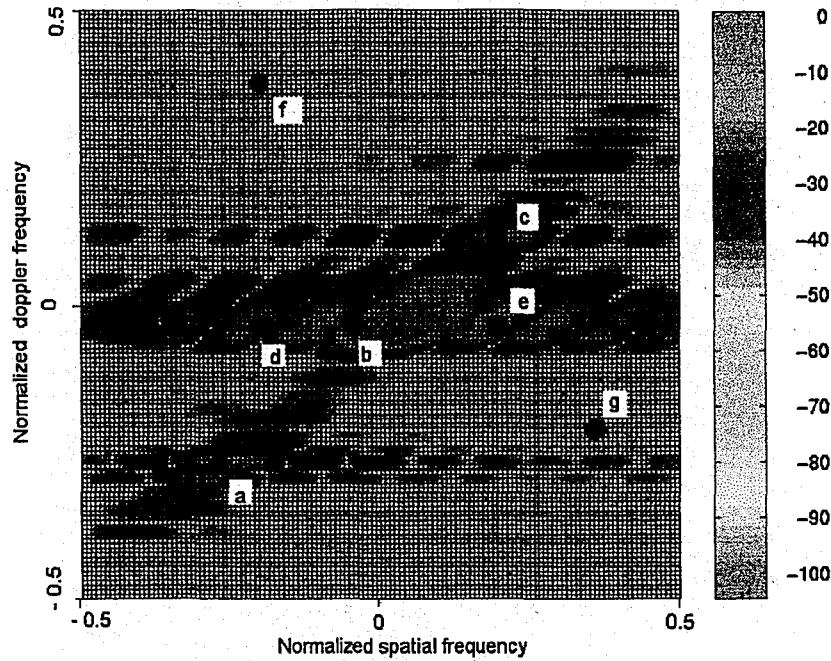


Figure 19) Power spectrum plot of range 500

Case	Normalized Doppler Frequency	Normalized Angle Frequency	The 3 best schemes	D
a	-0.2656	-0.2656	JDL EFA ADPCA	32 13 7
b	-0.0312	-0.0312	JDL EFA BEFA	22 20 15
c	0.125	0.203	JDL BEFA EFA, BeamAD	36 12 7
d	-0.0312	-0.1875	JDL EFA ADPCA	26 20 10
e	-0.0312	0.203	ADPCA JDL EFA	22 18 15
f	0.3593	-0.1875	JDL EFA, BEFA BeamAD	38 28 23
g	-0.1875	0.3593	BEFA, JDL BeamAD EFA	33 17 15

Table 5) The three best schemes for all the cases when the target is inserted at range 500. (D is the approximate difference between the normalized test statistic at the target peak and the largest peak in the normalized test statistic at some other range)

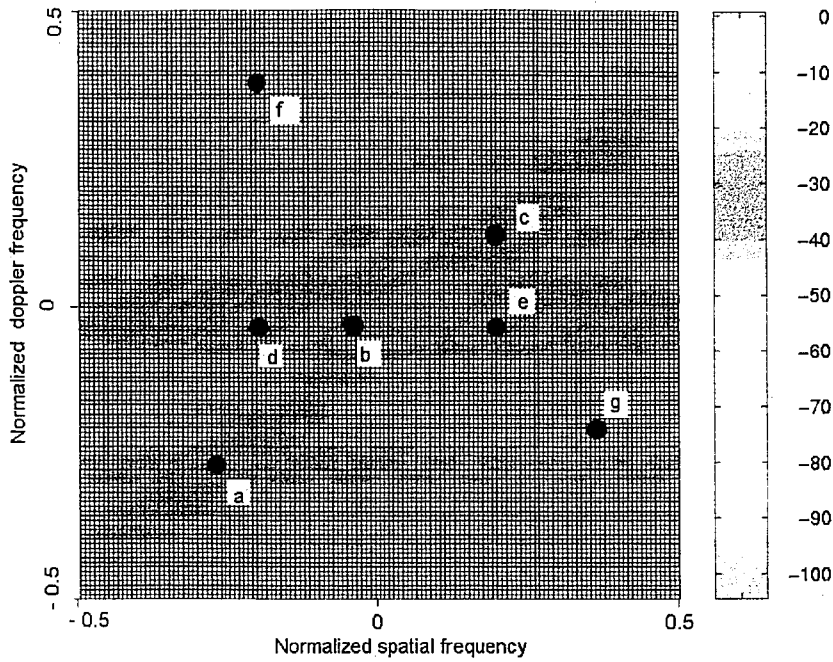


Figure 19) Power spectrum plot of range 500

Case	Normalized Doppler Frequency	Normalized Angle Frequency	The 3 best schemes	D
a	- 0.2656	- 0.2656	JDL EFA ADPCA	32 13 7
b	-0.0312	-0.0312	JDL EFA BEFA	22 20 15
c	0.125	0.203	JDL BEFA EFA, BeamAD	36 12 7
d	- 0.0312	- 0.1875	JDL EFA ADPCA	26 20 10
e	- 0.0312	0.203	ADPCA JDL EFA	22 18 15
f	0.3593	- 0.1875	JDL EFA, BEFA BeamAD	38 28 23
g	- 0.1875	0.3593	BEFA, JDL BeamAD EFA	33 17 15

Table 5) The three best schemes for all the cases when the target is inserted at range 500. (D is the approximate difference between the normalized test statistic at the target peak and the largest peak in the normalized test statistic at some other range)

Chapter 4

Conclusions

In our tests, JDL and EFA generally perform very well. Subarrayed EFA also shows good performance in many situations. The common element these schemes share is post Doppler processing. This type of processing, used in the correct way, appears to be superior in these real data cases. This appears to be the major result of this study. When there is a strong interference near the target, case d and e in Table 5 for example, ADPCA performs well and sometimes outperforms all the other schemes. The reason appears to be related to the extra whitening provided by its steering vector.

This is one of the few STAP studies we have seen which uses real airborne radar measurements and thus we feel these results are interesting. We acknowledge that judging performance using measured data is difficult since one can't directly extract probability of detection and probability of false alarm, the accepted measure of performance for radar signal detection problems. However, measured data studies are still important to obtain a more complete assessment of performance. In the current study we present comparisons only for a particular configuration of each algorithm, but we have tried to pick the most popular or at least a reasonable configuration for each algorithm. We acknowledge that the results may be different for different configurations. Further we have tested the algorithms for many different range

bins for two different data sets (flights) and based on these cases the results given here appear to be representative. However, we acknowledge that the results could be much different for some data sets we have not tested.

We have obtained results for a fairly large number of different cases. Due to space limitations we have provided only a limited set of results in this thesis. We believe that further study using measured data is needed and we hope to see more studies by other research groups on this topic. Hopefully other data sources will become available and these can be compared to results obtained using the MCARM database. We believe that techniques for assessing performance with measured data is itself a topic which deserves attention.

References

1. L.E. Brennan and I. S. Reed, " Theory of Adaptive Radar", *IEEE Trans. On Aerospace and Electronic Systems*, vol. AES-9, no. 2, pp. 237-252, March 1973.
2. I.S. Reed, J. D Mallett and L.E. Brennan, " Rapid convergence rate in adaptive arrays", *IEEE Transactions on Aerospace and Electronic Systems*, AES-10, no.6, November 1974.
3. A. Farina, *Antenna-based Signal Processing Techniques for Radar Systems*, (Artech House: MA, 1992).
4. H. Wang, Y. Zhang and Q. Zhang, "A view of current of space-time processing algorithm research", *IEEE International Radar Conference*, Alexandria, Virginia, May 1995, pp. 635-640.
5. J. Ward, *Space-Time Adaptive Processing for Airborne Radar*, Technical Report 1015, Lincoln Laboratory, 1995.
6. D. Sloper et. al., *MCARM Final Rept.*, Rome Lab tech. Rept., RL-TR-96-49, April 1996.
7. A. Oppenheim and R. Schafer, *Discrete-Time Signal processing*, Prentice Hall, Englewood Cliffs, New Jersey, 1989.
8. M. D. Zoltowski, "Beamspace M.L. Bearing Estimation for Adaptive Phased Array Radar", In *Adaptive Radar Detection and Estimation*, S. Haykin and A. Steinhardt Editors, John Wiley and Sons, New York, 1992.

9. R. C. Dipietro, "Extended Factored Space-Time Processing for Airborne Radar", Proceedings of the 2th Asilomar Conference, Pacific Grove CA, October 1992, pp. 425-430.
10. H. Wang and L. Cai, "On adaptive spatial-temporal processing for airborne surveillance radar systems", *IEEE Transactions on Aerospace and Electronic Systems*, Vol. 30, pp. 660-669, July 1994.
11. MCARM database web site - Rome Laboratory USAF, '<http://128.132.2>'.
12. L W. Melvin and B. Himed, "Comparative Analysis of Space -Time Adaptive Algorithms with Measured Airborne Data", presented at the 7th International Conference on Signal Processing Applications and Technology, October 7-10, 1996 .
13. W. Melvin, H.Wang and M. Wicks, "Multi-channel Airborne Radar Array Data Analysis", presented at 41st Annual Tri-Service radar symposium, June 1995.
14. H. Wang, "Space-Time Processing and Its Radar Applications", notes used for the class ELE 891 at Syracuse University, Summer 1995.

Biography

The author, Fatma B. Golbasi was born in Konya, Turkey. She got her BS degree in 1996, from the Electrical and Electronics Engineering Department of Bilkent University, Ankara. She started her Master's Program in spring 1997 at Lehigh University Electrical and Computer Engineering Department. Her research interests are Signal Processing, Telecommunications and Wireless Communication.

**END OF
TITLE**